Universidad del País Vasco
Euskal Herriko Unibertsitatea

ZTF-FCT
Zientzia eta Teknologia Fakultatea
Facultad de Ciencia y Tecnología

FACULTY OF SCIENCE AND TECHNOLOGY. LEIOA.

BACHELOR FINAL PROJECT CHEMICAL ENGINEERING

RESEARCH ON OPERATING CONDITIONS AT THE CATALYTIC REACTOR FOR THE COMBINED REMOVAL OF NO_X AND PCDD/PCDFs FROM MWI PLANTS

Student *Markaide Aiastui, Bittor Andoni*
Date *June 2015*

Director
Dr. Asier Aranzabal

Academic Year
2014/2015

TABLE OF CONTENTS

1 INTRODUCTION

The management of municipal solid waste (MSW), particularly the role of incineration, is currently a subject of public debate. Incineration shows to be a good alternative of reducing the volume of waste and eliminating certain infectious components. Moreover, Municipal Waste Incinerators (MWI), are reported to be highly hygienic (Hou, et al. 2014) and apart from that MWIs are immediately effective in terms of transport (incinerators can be built close to the waste sources) and incineration's nature.

Nevertheless, the emissions of many hazardous substances make the Municipal Waste Incineration (MWI) plants to be unpopular. Metals (especially lead, manganese, cadmium, chromium and mercury) are concentrated in fly and bottom ashes. Furthermore, incomplete combustion produces a wide variety of potentially hazardous organic compounds, such as aldehydes, polycyclic aromatic hydrocarbons (PAH), chlorinated hydrocarbons including polychlorinated dibenzodioxins (PCDD) and dibenzofurans (PCDF), and even acid gases, including NO_X. Many of these hazardous substances are carcinogenic and some have direct systemic toxicity.

In this regard, modern technology is able to meet current legislative limit values of emissions and the cost of operation of the solid waste's incineration can be offset by energy sales in waste to energy (WTE) thermal power plants (Brunner 1994). The measurement of concentration of the hazardous compounds in the exhaust flue gas of the MWIs is regulated by laws and requires certain periods of measurement as well as the compliance of limit concentrations shown in Table 1.1 and Table 1.2.

Table 1.1. *Gaseous compounds concentration limit values in MWI exhaust gases (Directive 2000/76/EC).*

Compound	Concentration, mg m^{-3}		
	Daily average	Half-hourly average	
		100%	97%
Total dust	10	30	10
Total organic carbon (gaseous)	10	20	10
HCl	10	60	10
HF	1	4	2
SO_2	50	200	50
NO_X (capacity > 6 T h^{-1} or new)	200	400	200
NO_X (capacity < 6 T)	400		

Table 1.2. *Metallic compounds limit concentrations in MWI exhaust gases (Directive 2000/76/EC).*

Metal (and it's compounds)	Concentration limit, mg m^{-3}	
	30 minutes average (minimum)	8 hours average (maximum)
Cd and Tl	0.05	0.1
Hg	0.05	0.1
Sb, As, Pb, Cr, Co, Cu, Mn, Ni and V	0.5	1

NO_X compounds have to be at least half-hourly measured and daily average values have to remain below 200 mg m^{-3}. NO_X formation rates are high enough to require a further treatment to comply legislation (Nakajima and Hamada, 1996).

Apart from the limits shown in Table 1.1 and Table 1.2 PCDD/PCDFs have to be measured over a sample in a period between 6 and 8 hours and concentration value must not be higher than 0.1 ng m^{-3}. Moreover, carbon monoxide should not exceed 50 mg m^{-3} daily average neither 150 mg m^{-3} average of 95% of measurements in 10 minutes average or 100 mg m^{-3} in average half-hourly measurements over 24 hours (Directive 2000/76/EC). To ensure the compliance of the set limits most of the countries oblige MWIs to have on-line analyzers of CO, CO_2, HCl, SO_2, NO_X, total hydrocarbons, particulates, water content and O_2 while the rest of the components are usually measured offline (McKay 2002).

In order to comply the legislative limits and to discharge the minimum quantity of hazardous compounds, MWIs are equipped with post-combustion Air Pollution Control Devices (APCDs) which commonly include (different technologies might be applied in each MWI plant):

-Electrostatic precipitator for elimination of particles.

-Fabric filters for the elimination of solid PCDD/PCDFs and vapours associated with particles.

-Dry and wet scrubbers to remove acid gas and particles.

-Dry sorbent injection to reduce acid gas emissions.

-Entrained flow adsorber which recirculates an adsorbent until it is exhausted and burned.

-Circulating fluidised bed of fine-grained heat-oven coke and an additive that can simultaneously absorb HCl, HF and SO_2.

-Moving-bed adsorber which is used as an alternative for fixed bed adsorbers that can be blocked due to moisture.

-Selective catalytic reactor for elimination of NO_X.

The research of more effective methods for the removal of the pollutants from exhaust gases has become essential since, besides the environmental effects, laws are becoming increasingly strict, especially regarding to emission, requiring lower concentrations and harmfulness in exhaust gases (Directive 2000/76/EC).

1.1 STATE OF THE ART OF REMOVAL OF POLLUTANTS

Nowadays most usual technology, even if its usage is decreasing, is the non-catalytic reaction with ammonia for the abatement of NO_X while PCDD/PCDFs are set aside by physical containment methods like the activated carbon filters.

Addition of ammonia to the waste combustion chamber leads to transformation of NO_x compounds in N_2. This technique is out-dated for the required emission limits (Directive 2000/76/EC) what has caused the use of a more effective technique which is the selective catalytic reduction (SCR). Worldwide municipal waste incinerator (MWI) plants have begun to apply this state-of-the-art technique recently with the use of V_2O_5-WO_3-TiO_2 as catalyst which has shown a very good performance for NO_x SCR with ammonia. In this context, it is reported that the SCR reaction occurs in parallel with many other competitive reactions creating unwanted products. (Busca, et al. 1998).

Authors agree that the SCR reaction stoichiometry is the following:

$$4\ NH_3 + 4\ NO + O_2 \rightarrow 4\ N_2 + 6\ H_2O \qquad (1)$$

Where it has been demonstrated that one atom of N_2 comes from NO and the other from NH_3, but also another reaction path has been reported (Goemans, et al. 2003):

$$8\ NH_3 + 4\ NO + 2\ O_2 \rightarrow 6\ N_2 + 12\ H_2O \qquad (2)$$

Moreover, in absence or defect of oxygen reaction (1) turns into:

$$4\ NH_3 + 6\ NO \rightarrow 5\ N_2 + 6\ H_2O \qquad (3)$$

Also a selective reduction of NO_2 has been reported in V_2O_5 catalysts:

$$4\ NH_3 + 2\ NO_2 + O_2 \rightarrow 3\ N_2 + 6\ H_2O \qquad (4)$$

Nevertheless, other non-selective unwanted reactions are also reported, consuming ammonia or giving rise to unwanted products:

$$4\ NH_3 + 4\ NO + 3\ O_2 \rightarrow 4\ N_2O + 6\ H_2O \qquad (5)$$

$$4\ NH_3 + 3\ O_2 \rightarrow 2\ N_2 + 6\ H_2O \qquad (6)$$

$$2\ NH_3 + 2\ O_2 \rightarrow N_2O + 3\ H_2O \qquad (7)$$

$$4\ NH_3 + 5\ O_2 \rightarrow 4\ NO + 6\ H_2O \qquad (8)$$

Ammonia can also be consumed in an unwanted reaction that takes place in presence of HCl which is formed by the oxidation of PCDD/PCDFs as explained later. As a product ammonium chloride is formed, a crystalline salt that can obstruct conducts:

$$NH_3 + HCl \rightarrow NH_4Cl \qquad (9)$$

PCDDs and PCDFs are exhausted from MWI in the flue gases, in the fly ash and in the slag. It has been reported that the pollution controlling systems are enough to remove the 99% of

the PCDD/PCDFs in solid the residues. On the other hand, the dioxins and furans present on the flue gases are set aside from the rest of gases by dry adsorption technique and also wet scrubbing is an effective way (98%) of treatment. However, these adsorption- and absorption-based techniques transfer PCDD/PCDFs from gas phase to solid or liquid phases which require further intertization treatments. That's why catalytic technologies are preferable for their removal at the source of emission through Catalytic Total Oxidation (CTO), destructing hazardous molecules which form carbon oxides and HCl as shown hereafter. (Finocchio, et al. 2006; Goemans, et al. 2003; McKay 2002; Debecker, et al. 2007).

$$C_{12}H_nCl_{8-n}O_2 + (9+0.5\ n)\ O_2 \rightarrow (n-4)\ H_2O + 12\ CO_2 + (8-n)\ HCl \qquad (10)$$

$$C_{12}H_nCl_{8-n}O + (9.5+0.5\ n)\ O_2 \rightarrow (n-4)\ H_2O + 12\ CO_2 + (8-n)\ HCl \qquad (11)$$

It is noteworthy that catalytic technologies enable a effective oxidation between 250 ºC and 550 ºC and show a good oxidizing performance for low concentration strings without additional fuels (Wu, et al. 2012).

1.2 SIMULTANEOUS REMOVAL OF NO_X AND PCDD/PCDFS

Catalytic technologies for elimination of NO_X through NH_3-SCR have been widely studied with VO_X/TiO_2 catalysts (Busca, et al. 1998). It has been found out that VO_X/TiO_2 catalysts, which are commercially used for the abatement of NO_X by SCR, are also suitable for the removal of PCDD/PCDFs (Wang, et al. 2015; Wielgosinski, et al. 2007; Wu, et al. 2012; Krishnamoorthy et al. 1998; Debecker, et al 2007; Albonetti, et al. 2008). The removal of NO_x and PCDDs / PCDFs, denoted as deNOx and deDin reactions, has been proved to be possible forming a deDiNox system using catalytic technology, but there is not many literature about it yet (Gallastegi-Villa, et al. 2015; Jones and Ross 1997; Goemans, et al. 2003; Xue, et al. 2013; Su, et al. 2015). Nevertheless, there are other researchers who have studied the field and the effect of the presence of NO in the abatement of PCDD/PCDF models through oxidation (Dvorák, et al. 2010; Bertinchamps, et al., 2005).

Different dispositions are possible to set the deDiNox system. In order to avoid further de-novo formation of PCDD/PCDFs, the so called Tail-End (Figure 1.1) disposition is the best one, since no high temperatures are applied once passed the deDiNox unit. However, the flue gas temperature is around 180 ºC and therefore the gas needs to be re-heated in order to achieve the optimum catalytic temperature, which is about 300 ºC for commercial $V_2O_5/WO_3/TiO_2$ catalyst. (Forzatti, et al. 2012; Gallastegi-Villa, et al. 2015; Krishnamoorthy, et al. 1998; Nakajima and Hamada, 1996; Wielgosinski, et al. 2007).

In the shown system in Figure 1.1, particles and ashes and HCl, SO_2 and HF would be eliminated in the particle precipitation and adsorption installations. The catalytic reactor would carry out the deDiNox process.

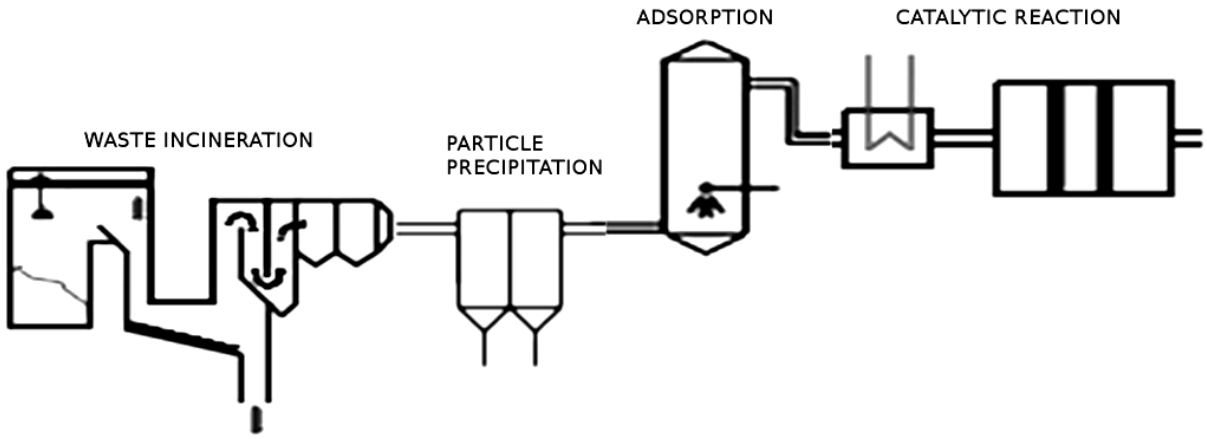

Figure 1.1. *Tail-End disposition of the deDiNox system.*

1.3 MODEL COMPOUNDS

The experimental study of polluted gas strings involves exposure to risky atmospheres. Because of that, less toxic are chosen to simulate the most hazardous compounds.

On the one hand, NO_X gases can easily be simulated by NO which is the one that shows the highest concentration (Busca, et. al. 1998; Dvorák, et al. 2010).

On the other hand, there is a wide diversity on the different types of dioxins and furans that can be found in the MWI exhaust gas. In order to get a valid and comparable concentration unit, each variety of PCDD or PCDF has its own toxic equivalent (different for each standard model), that is to say, the toxicity relation between it the most toxic known dioxin: 2,3,7,8-tetrachlorodibenzodioxin (2,3,7,8-TCDD). In scientific studies model compounds are used, which have to be structurally similar to PCDD/PCDFs, less toxic and easier to handle. Catalytic activity has been evaluated in the oxidation of the aromatic ring as well as resistance to chlorine poisoning. In this regard, the most studied compound for research with PCDD/PCDFs is 1,2-dichlorobenzene or ortho-dichlorobenzene (o-DCB). Structural similarities are shown in Figure 1.2. (Debecker, et al. 2007; Krishnamoorthy, et al. 1998; McKay 2002).

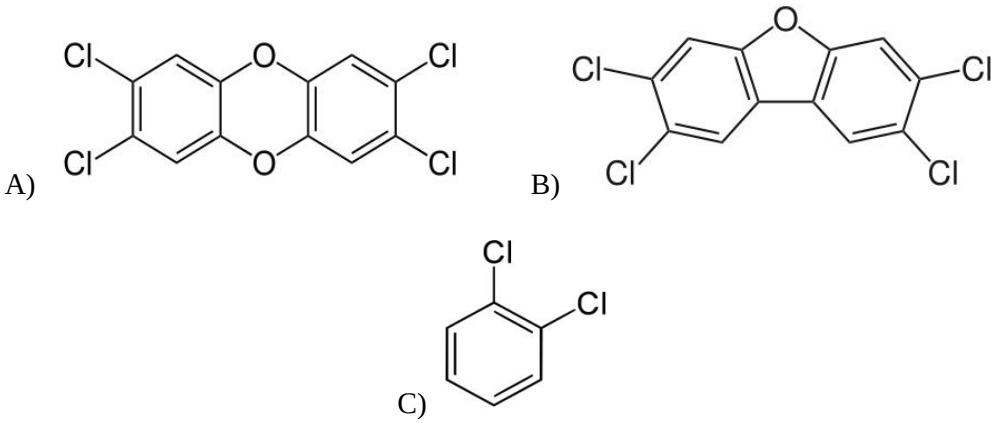

Figure 1.2. *Molecular structures of 2,3,7,8-tetrachlorodibenzodioxin (A), 2,3,7,8-tetrachlorodibenzofuran (B) and 1,2-dichlorobenzene (C).*

1.4 VO_X/TiO_2 CATALYST

Vanadia-based catalysts are industrially applied for instance in NO_X reduction (NH_3-SCR) as V_2O_5-WO_3/TiO_2 or V_2O_5-MoO_3/TiO_2 (Wang, et al. 2015). It has also been proved that vanadium-tungsten and vanadium-molybdenum catalysts are suitable for the decomposition of PCDD/PCDFs, and also resistant against deactivation (Bertinchamps, et al. 2005).

TiO_2 is frequently used as a support or carrier for showing catalytic activity and good mechanical, thermal and anticorrosive properties (Gannoun, et al. 2012; Wielgosinski, et al. 2007). Although there is not much literature about the effect of the phase of the support in the catalytic performance (Wu, et al. 2012), improved activity is reached using highly crystalline titania, which increases the dispersion of vanadia in the support (Economidis, et al. 1999).

Interaction between vanadia and titania result in amorphous monomeric (isolated) or polymeric VO_X species than can be formed in sub-monolayer coverage (< 7-8 V atoms nm^{-2}). Polymeric species are formed by the attachment of monomeric species through V-O-V bonds. With higher loadings, crystalline V_2O_5 species appear from highly polymerized species, which is considered to have detrimental effects on catalytic activity, regardless the preparation method. (Schimmoeller, et al. 2010; Gallastegi-Villa, et al. 2015).

In the simultaneous abatement of NO and o-DCB, it is reported that the isolated VO_X species are the most active for the oxidation of o-DCB, whereas polymeric ones show a better performance for the NO reduction (Gallastegi-Villa, et al. 2015).

2 OBJECTIVES

The main goal of this project is to determine the effect of operating variables in order to obtain a mechanistic equation. Concretely, it is expected to study which is the effect of the different compound's concentrations in the simultaneous SCR of NO_X and CTO of PCDD/PCDFs in a MWI performed over a VO_X/TiO_2 catalyst.

For the compliance of the main objective, the following milestones are posed:

Preparation of the VO_X/TiO_2 catalyst and its characterization in order to check that properties were adequate.

Determination of reaction conditions for a reactor free of mass and heat transfer's effects. Assessment of theoretical criteria and evaluation of agreement with experimental results.

Selection of reaction conditions (Temperature, catalyst's mass, space time, ...) to obtain suitable and representative experimental results.

Calculation of the x_A *vs.* W/F_{A0} curve to obtain a empirical expression of reaction rate.

Proposal of a mechanistic reaction rate's equation including influences of the reactions on each other.

3 MATERIALS AND METHODS

This section describes how the catalyst samples were prepared, the methods used for the characterization and the conditions for catalytic tests. The whole reaction system and conditions for measurements are also described.

3.1 CATALYST'S PREPARATION

VO_X/TiO_2 catalyst was prepared through classic wet impregnation method. Titania (TiO_2) in anatase phase was supplied by Millenium Inorganic Chemicals' - Cristal Global (Cristal ACTiVTM G5). It was calcined at 550 ºC for 3 h to be used as the catalyst's support. VO_X was obtained from NH_4VO_3, ammonium metavanadate, supplied by Sigma-Aldrich, 99.99%.

Impregnating solution was obtained by dissolving the necessary amount of precursor for a 3% load of vanadium with distilled water, and adding the necessary quantity of oxalic acid (Sigma-Aldich, 99.99%) for a 2:1 molar relation to obtain aged vanadia (V^{4+}) species in impregnation solution, which have been reported to perform better (Economidis, et al. 1999). The vanadium loading was fixed on 3% in order to obtain a nearly monolayer coverage of VO_X over TiO_2, since it has been proved it has the loading with the best catalytic performance (Gallastegi-Villa, et. al 2015; Wang et al. 2015). After being stirred enough to obtain a homogeneous solution, all the water was evaporated in a rotary evaporator apparatus, at 35 ºC and 3 mmHg. Samples were dried overnight at 110 ºC and later calcined in air at 500 ºC for 3 h (1 ºC min^{-1}).

Before being used, the mass was stirred to homogenize the composition. The catalyst was pelletized, crushed and sieved to different particle sizes.

3.2 CATALYST'S CHARACTERIZATION

3.2.1 Chemical composition

The actual amount of V and Ti on the prepared samples was characterized by Inductive Coupled Plasma, ICP-AES (Horiba Jobin Yvon, Activa). A sample of the powdered catalyst was dissolved with a 1:3 molar solution of HNO_3:HCl, nitric acid to hydrochloric acid, and a few drops of HF, hydrofluoric acid, were added to obtain a complete disintegration at 90 ºC.

3.2.2 Textural properties

The textural properties of the catalyst were evaluated by N_2 adsorption-desorption at -196ºC in a Micromeritics TRISTAR II 3020 apparatus. The treated samples of 200-800 mg were degassed for 4 h at 350 ºC under a nitrogen flow. The specific surface area was measured by standard Brunauer-Emmett-Teller (BET) procedure using the data of adsorbed nitrogen measured in the range of partial pressure (P/P_0) of 0.03-0.3. Average pore size and distribution was calculated by the Brunauer-Joyner-Halenda (BJH) method using the desorption isotherms.

3.3 REACTION SYSTEM

The experimental set-up flow diagram is shown in Figure 3.1. Reaction feeding was a simulated MWI flue gas. Nominal concentration values were the ones shown in Table 3.1.

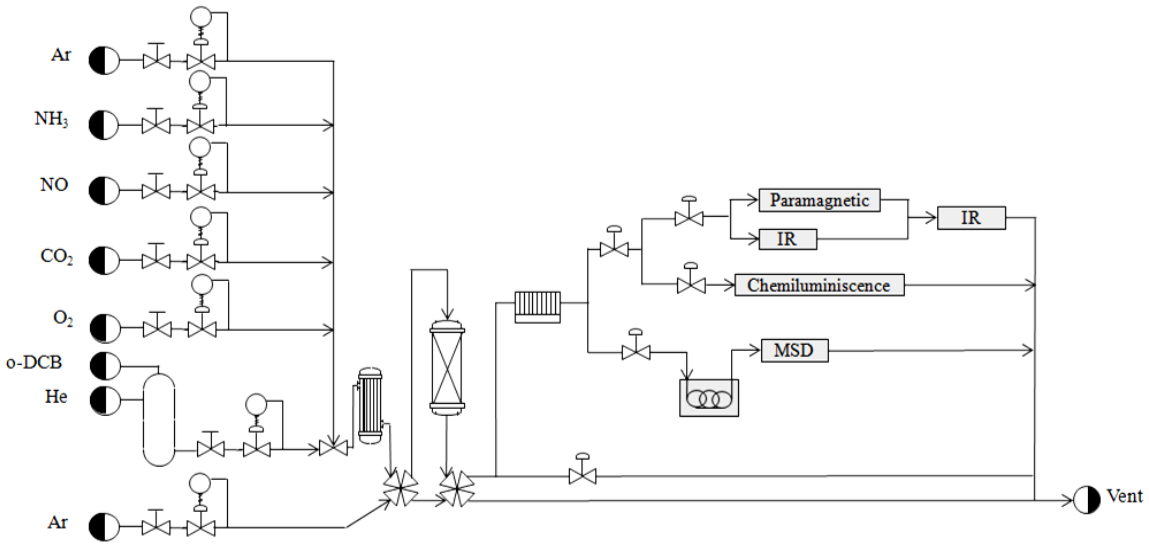

Figure 3.1. *Reaction system set-up.*

Table 3.1. *Nominal concentration values in feeding.*

Compound		Concentration
Nitrogen monoxide	NO	300 ppm
Ammonia	NH_3	400 ppm
Carbon dioxide	CO_2	10% (vol.)
Oxygen	O_2	10% (vol.)
Ortho-dichlorobenzene	o-DCB	100 ppm
Argon	Ar	balance

The gas flows (Ar, NO, NH_3, O_2, CO_2) were regulated by gas mass flow controllers (Bronkhorst® High-Tech F-201CV), whereas o-DCB liquid stream was dosed by a Bronkhorst® High-Tech μ-Flow L01-AAA-99-0-20S mass flow controller.

Liquid was pressurized with Helium. The complete evaporation of the liquid and homogeneous blend of components was accomplished in a Bronkhorst® High-Tech W-102A-111-K controlled-evaporator-mixer (CEM). Furthermore, all pipelines were heated with electrical resistances to avoid gas adsorption or condensation.

The resulting gaseous stream went through the fixed catalytic bed in a U-shaped tubular quartz reactor (13.6 mm i.d.) located inside convective-flow oven. The fixed bed was mounted over calcined quartz wool and was composed by the given catalyst's mass and crushed and sieved inert quartz to fill 2 cm^3 volume so that the GHSV would not depend on the quantity of catalyst for each reaction. Reaction's products went through a filter, to avoid obstruction of the piping or analyzers. Two four port valves allowed the feed to bypass the reactor and go directly to analyzers or expel it to atmosphere. An auxiliary Ar stream was also set parallel to feed system in order to dry the catalyst before the reaction and to clean tubbing.

Reactor outlet stream was divided and fed to three inlets for composition's analysis. The first sub-stream was fed to an Agilent Technologies 7890A on-line gas chromatograph equipped with HP-VOC capillary column and a mass selective detector (MSD) 5975C was used to measure o-DCB concentration in the reactor inlet and outlet streams. The second sub-stream was fed to NGA 2000 Rosemount Analytical analyzers where O_2 was measured by a paramagnetic detector and CO_2, CO and N_2O were analyzed by infrared (IR). The outlet stream of the NGA 2000 Rosemount Analytical analyzers was connected to a XStream gas analyzer where concentration of NH_3 was measured by IR. The third sub-stream was fed to a NGA 2000 CLD chemiluminiscence detector (CLD) which measured NO concentrations. All analyzer outlets were afterwards rejoined and sent to vent.

All reactions were carried out as steady state reactions. Experimental error resulted in variation of data in time, which's effect was studied by the standard deviation.

When setting up a reaction, the feeding was created first. When stabilized, it was analyzed by the analyzers. Meanwhile, the catalyst's fixed bed was dried at 200 ºC for at least 2 hours in pure Ar (auxiliary) flow of 2 l_S min^{-1} (GHSV = 60000 h^{-1}).

3.4 REACTIONS DESIGN

The experimental reactions' conditions and characteristics are explained in this section. Procedures are described for the setting of the conditions of the kinetic study and the reactions for the kinetic study itself.

3.4.1 Diffusion's analysis

Heterogeneous catalytic reactions happen in different stages. Reagents have to cross firstly the boundary layer around the catalyst particle to reach the surface of the particle and hereafter travel through the pore to an active site, upon which the chemical processes take place as it is shown in Figure 3.2. The reaction products must do the same way back after being desorbed from the active site. Therefore, when analyzing a heterogeneous catalytic process's kinetic mechanism there is need of ensuring that the chemical stage is the slowest stage of the whole process. In such condition, an intrinsic kinetic regime is set, that is to say, external and internal physical diffusion of reagents happen so fast that their effect can be negligible. This section will set the conditions for the following tests.

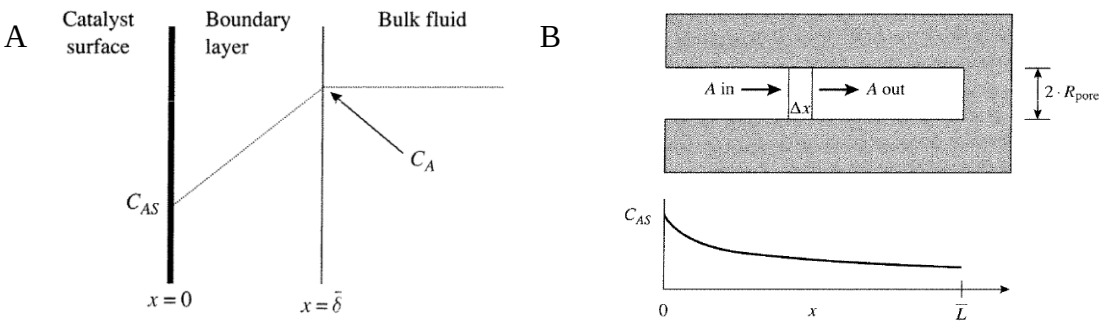

Figure 3.2. *External (A) and internal (B) diffusion of reagents in heterogeneous catalytic reactions.*

Conditions for the catalytic reactions have to be cautiously chosen to comply the requirements of the process for a intrinsic kinetic regime. Size of catalyst's particles or linear velocity of reagents are, parameters to take into account among others.

3.4.1.1 External diffusion

External diffusion will be negligible when the linear velocity of reagents is high enough to wipe out the stagnant boundary layer being any concentration gradient between the catalyst's surface and the reagents flow eliminated. A mass balance in the boundary layer of the interfacial surface (Figure 3.2 (A)) equals the transferred moles to catalyst's surface, proportional to the concentration gradient, and the reaction rate (Davis 2003):

$$-r_A \rho_C = k_C (C_A - C_{AS}) a_m \qquad (12)$$

When concentration gradient over the film is less than a critical value, it is considered that the reactor is free of external diffusion's resistances.

Since the mass transfer coefficient is primarily function of the linear velocity ($k_C \propto u^{0.5}/d_p^{0.5}$) (Fogler 2005) of the gas flow an easy way to check external difussional resistances is to record the reaction rate by increasing the linear velocity or the volumetric flow rate, by keeping in a constant space time value (W/F_{A0}), low enough to consider a differential reactor. As a result, the minimum linear velocity will be calculated when constant conversion values are obtained for different flow rates. Conversion was calculated as a percentage of reacted moles over introduced:

$$x_A = \frac{C_{A0} - C_A}{C_{A0}} \cdot 100 \qquad (13)$$

Alternatively, a variety of criteria have been proposed based on this assumption, for example Mears' criterion (Mears 1971). According to it, the compliance of the following condition ensures the absence of external mass transfer control on an irreversible, isothermal, power law kinetic reaction in a spherical catalyst pellet.

$$\frac{(-r_A)_{obs} \rho_L r_P n}{k_c C_A} < 0.15 \qquad (14)$$

3.4.1.2 Internal diffusion

Internal diffusion is the one that takes place in the catalysts' pores. A mass balance can be deduced from Figure 3.2 (B) for a first order power law reaction, in a Δx thickness:

$$k_S C_A (2 \pi R_{Pore}) (\Delta x) = \pi R_{Pore}^2 N_{A,x} - \pi R_{Pore}^2 N_{A,x+\Delta x} \qquad (15)$$

The shorter a pore is, the sooner mass transfer will happen and the less probable will be a concentration gradient inside the pore. In this regard, since smaller particle have shorter pores, they are more likely to avoid slow mass transfer rates in the pores, since active sites are closer to the surface, while bigger particles hinder mass transfer.

Chemical reaction rate and diffusion rate are compared in Weisz-Prater criterion (Green and Perry, 2008). A lack of intraphase diffusion effects on an irreversible, isothermal power law kinetics reaction in a spherical catalyst pellet can be assessed with the compliance of:

$$\frac{(-r_A)_{obs}\,\rho_C\,r_P^{\,2}}{D_E\,C_A} < 1 \qquad (16)$$

That is to say, when diffusion rate is higher than the rate of chemical reaction.

The checking of internal diffusion's effects was carried out by sieving particles to different sizes and then taking them into reaction under equal conditions. Reactions were carried out at constant flow rate, space time and temperature. Internal diffusion's effect was neglected when same conversion was obtained for different size particles.

3.4.1.3 Heat transfer

Temperature gradients' effects are decisive in kinetic research. Effect of heat transfer has to be measured in the temperature gradients of the catalyst's particles. That is too difficult to do experimentally so an empirical estimation was carried out by calculating the effect of the chemical process's reaction heat in the gradient of temperature between the catalyst particle and the gas flow. That way, the effect of the heat generated in a catalyst's particle in the rest of the catalytic bed is also evaluated.

Apart from that, temperature in the catalytic bed's inlet and temperature in the reactor outlet (right after the catalytic bed) was measured in steady-state conditions with a double point thermocouple. That way the effect of the reaction heat in the bed's temperature was observed, and how isotherm the reactor is was evaluated.

3.4.2 Effect of compounds' concentrations in both reactions

The main objective of this research was to be able to predict the reactions' behaviour under different conditions. Those conditions, dependent on the different possible composition of feed, which in reality would be the different composition of a MWI effluent gas, were performed in the reactor.

Reactions varying the concentrations of NO-NH_3, o-DCB and O_2 and the influence of the possible different NO:NH3 ratio in the reactor feed were carried out to study the effect of the absence or presence at different concentrations. The effect of the different reaction conditions was measured by quantifying conversion of reactants and selectivity to different products. Selectivity, defined as the concentration of a product in relation with the maximum stoichiometrically possible from the reacted quantity, was calculated for different products by the following formulas:

Selectivity of o-DCB towards CO:

$$S_{CO} = \frac{C_{CO}}{x_{o\text{-}DCB}\cdot C_{0,\,o\text{-}DCB}\cdot 6\left(\dfrac{mol_C/mol_{o\text{-}DCB}}{mol_C/mol_{CO}}\right)}\cdot 100 \qquad (17)$$

Selectivity of o-DCB towards CO_2:

$$S_{CO_2} = \frac{C_{CO_2}}{x_{o\text{-}DCB} \cdot C_{0,\,o\text{-}DCB} \cdot 6 \left(\frac{mol_C / mol_{o\text{-}DCB}}{mol_C / mol_{CO_2}} \right)} \cdot 100 \qquad (18)$$

Selectivity of NO towards N_2O:

$$S_{N_2O} = \frac{C_{N_2O}}{x_{NO} \cdot C_{0,NO} \cdot 0.5 \left(\frac{mol_N / mol_{NO}}{mol_N / mol_{N_2O}} \right)} \cdot 100 \qquad (19)$$

4 RESULTS AND DISCUSSION

4.1 CATALYST'S CHARACTERIZATION

Prepared catalyst's properties were checked and compared to those reported in literature in order to ensure the catalyst was properly prepared and that its properties were the expected.

Composition of catalyst was obtained through ICP analysis of three different samples. An average vanadium loading of 3.33% (wt.) was achieved with a Relative Standard Deviation (RSD) of the 6.9% between different samples, and 59.41% titanium (RSD 2.6%). The deviation from the nominal value can be justified with the different errors that can accumulate from preparation of the catalyst to the performance of the analysis (very little quantities, about 0.02 g, are being theoretically totally disintegrated) apart from the inaccuracy of the analysis equipment itself.

N_2 adsorption of the bare TiO_2 support (Figure 4.1) support showed a characteristic shape of mesoporous solids type IV, according to IUPAC where adsorption takes place forming multiple layers. This is the reason why isotherms' slope is close to zero in the middle of partial pressure range, and highly positive for lowest and highest partial pressures. Moreover, type IV isotherms show a characteristic hysteresis phenomena since when filling the pores during adsorption, the required relative pressure is that correspondent to the pore while the emptying (during desorption) happens in the correspondent relative pressure of the pore's throat. The calculated average BET surface area of the support was 60.0 m^2 g^{-1} for different samples, with a RSD of 0.4%. The pore distribution is shown in Figure 4.2. It is a bimodal distribution with the peaks centred around 23 Å and 90 Å pores, where the second ones are predominant.

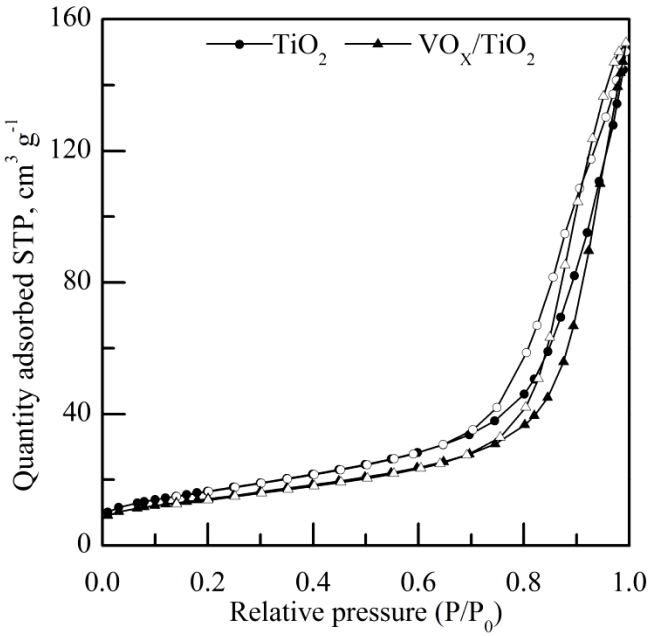

Figure 4.1. *N_2 adsorption (Filled) and desorption (Empty) isotherms.*

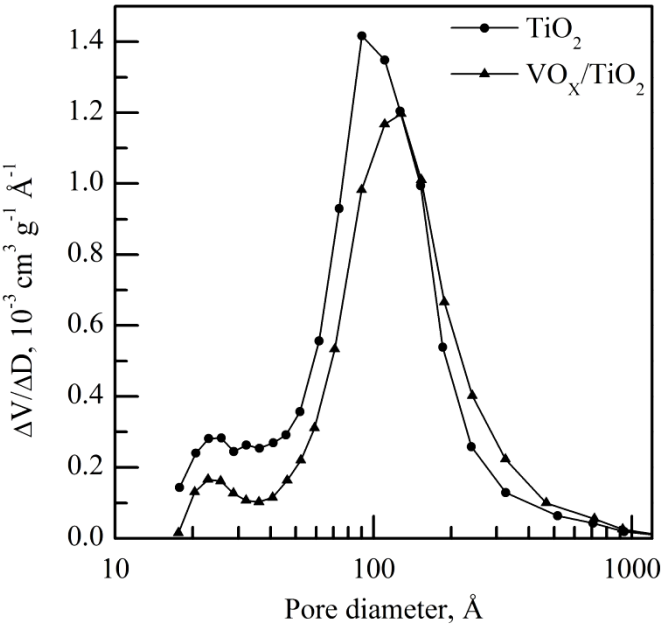

Figure 4.2. *Pore distribution.*

After impregnation and calcination, 0.20 mm sized samples (the used ones for the kinetic study in the further sections) showed an average BET surface area of 50 m^2 g^{-1} (RSD 3.13%), a close value to those reported by (Wu, et al. 2012; Debecker, et al. 2007; Wang, et al. 2015). A decrease of 16,7% was observed, which has been previously reported (Albonetti, et al. 2008; Gallastegi-Villa, et al. 2015; Wang, et al. 2015) to occur nearly proportional with the vanadium loading.

Adsorption isotherm's shape did not change after vanadia loading and it was also considered as a type IV solid as it is shown in Figure 4.1. Pore distribution was also bimodal although mainly centred in 100 A. In addition, less pores were observed in the impregnated sample due to the loss of specific surface area.

4.2 INTRINSIC KINETICS CONDITIONS DETERMINATION

This section is focused on the analysis of mass and heat transfer's effects, described in section 3.4.1. In this regard, conditions for a intrinsic kinetic reaction system are obtained in order to design further experimental reactions to obtain a mathematic expression for the reaction rate.

4.2.1 Experimental results

4.2.1.1 Mass transfer's effect

The aim of this section is to obtain experimental limits for the further kinetics study. Remaining reaction conditions in compliance with these limits, no other reaction rate than the chemical stages' will be observed, that is to say, mass transfer will happen that fast it's effect in the observed reaction rate will be negligible.

The chemical reaction's fastest speed will be observed in the limit space time value. Any faster reaction rate (implying a lower space time) will not ensure the absence of mass transfer's limitation, since if chemical reaction happens faster diffusion stages can become

slower, thus, more likely to be limiter. The lowest possible W/F_{A0} and conversion values are looked forward, involving high reaction rates, to allow a wide range of space time in intrinsic kinetic regime. That is interesting for the next part of the experimentation when different concentrations will be performed for different.

Choice of temperature was carried out through values of conversion at different temperatures. Results obtained with 0.2 mm particle size catalyst are shown in Figure 4.3 for different temperatures. All reactions were carried out at constant residence time (W/F_{A0}) of 311 g h mol^{-1} for NO and 933 g h mol^{-1} for o-DCB with a flow rate of 2 l_S min^{-1} and using 0.5 g of catalyst.

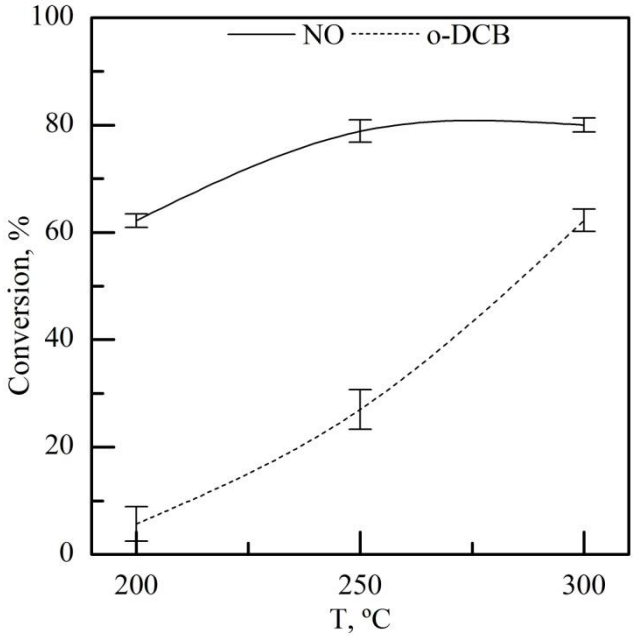

Figure 4.3. *Conversion in different temperatures (d_P: 0.2 mm, Q: 2 l_S min^{-1}).*

Figure 4.3 shows the conversion of NO by SCR and o-DCB by CTO when both reactions happen simultaneously in the reactor. Conversion of NO is significantly higher in the experimented temperature range, for instance, when conversion of 60% was obtained for NO, less than 10% was reached for o-DCB in the same conditions (200 ºC). The following reactions were performed at 200 ºC and 250 ºC, to obtain conversion data of NO and o-DCB respectively.

Internal mass transfer was theoretically calculated to be more restrictive than external (section 4.2.2). Because of that, internal mass transfer was studied firstly, although external mass transfer takes place before in the reaction. Reactions were carried out at two different space time values, using 0.3g and 0.5g of catalyst. Reaction conditions are summarised in Table 4.1.

Table 4.1. *Reactions' conditions for internal mass transfer evaluation.*

Parameter	Value		
d_P, mm	0.21	0.40	0.65
Q, l_S min^{-1}	2		
W, g	0.3		0.5
$u_{200\ ºC\ (NO)}$, m s^{-1}	0.27		0.27
$u_{250\ ºC\ (o\text{-}DCB)}$, m s^{-1}	0.29		0.29
$W/F_{0,\ NO}$, g h mol^{-1}	187		311
$W/F_{0,\ o\text{-}DCB}$, g h mol^{-1}	560		933

Obtained results are shown in Figure 4.4.

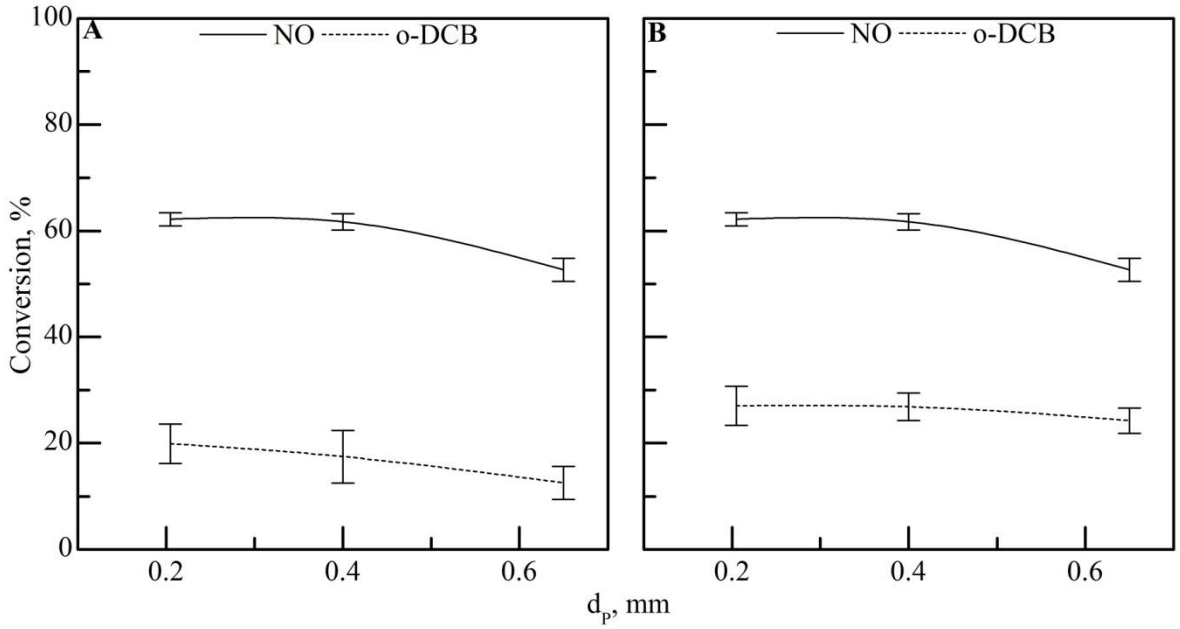

Figure 4.4. *Conversion with different particle diameters at different catalyst's mass: A) 0.3 g and B) 0.5 g.*

As expected, higher conversions were reached for both reactants at higher space times, specially in o-DCB oxidation reaction.

Analysis of o-DCB showed higher deviation than NO's, what is more in low conversions. Therefore, due to uncertainty at low conversions, values obtained using 0.5 g of catalyst were used for comparison.

Conversion did not change for NO nor for o-DCB using 0.2 or 0.4 mm particles. In contrast, conversion of NO decreased significantly, so did the o-DCB's, although more slightly, when using particles of 0.65 mm. The decrease of conversion was attributed to presence of

diffusion's effects. Therefore, catalyst particles sieved to 0.2 mm were used in further reactions, ensuring a system free of internal diffusion's effects.

External mass transfer was studied by using different linear velocities. In the experimental equipment, volumetric-flows were introduced as input, and this way linear velocities were modified. Space time was kept constant. Reaction conditions are summarised in Table 4.2.

Table 4.2. *Reactions' conditions for external mass transfer evaluation.*

Parameter	Value		
d_P, mm		0.2	
W, g	0.375	0.5	0.625
Q, l_S min^{-1}	1.5	2	2.5
$u_{200\ ºC\ (NO)}$, m s^{-1}	0.20	0.27	0.33
$u_{250\ ºC\ (o\text{-}DCB)}$, m s^{-1}	0.22	0.29	0.36
$W/F_{0,\ NO}$, g h mol^{-1}		311	
$W/F_{0,\ o\text{-}DCB}$, g h mol^{-1}		933	

Results for the reactions carried out at different volumetric flow rates are shown in Figure 4.5.

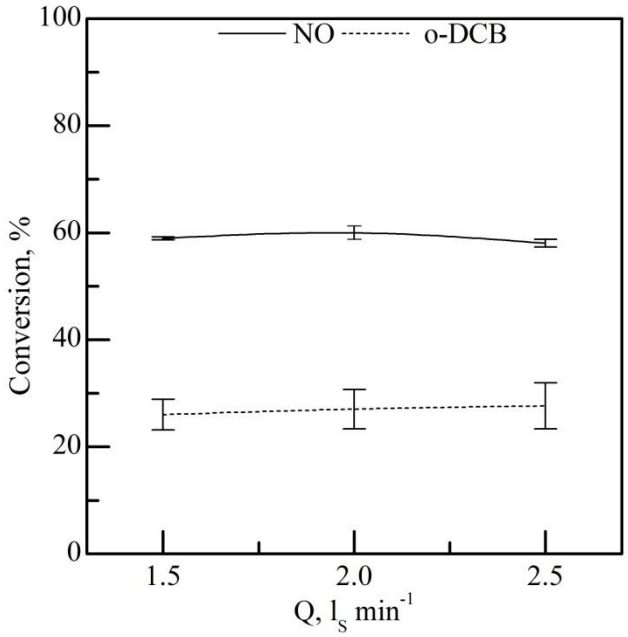

Figure 4.5. *Conversion values for different flow rates.*

Similar conversion values were observed in the three different flow rates. Therefore, using 1.5 l_S min^{-1} (linear velocities of 0.2 m s^{-1} at 200 ºC and 0.22 m s^{-1} at 250 ºC) or a higher flow rate at given conditions, reaction's conversion nor rate would vary. Thus, external diffusion's

effect would be negligible, and constant concentration of reagents could be considered between the bulk flow and the catalyst's surface.

Conditions were set for further reactions where particles of 0.2 mm would be used for reactions with higher volumetric flow rates than 1.5 l_S min^{-1} in the reaction system, in other words, linear velocities above 0.2 m s^{-1} at 200 ºC (for the SCR) and 0.22 m s^{-1} at 250 ºC (for the CTO). In further performances with different inlet concentrations would always be ensured higher space time values than 311 g h mol^{-1} for NO and 933 g h mol^{-1} for o-DCB.

4.2.1.2 Heat transfer's effect

Reaction heat's effect in temperature gradients was experimentally turned down by measuring temperature in the fixed bed inlet and in the outlet at different set point temperatures by either feeding an inert gas (Ar) and reaction composition with a double thermocouple. Reactions were carried out with variable volumetric flows between 1.7 and 2.7 l_S min^{-1} with a composition of 100 ppm o-DCB, 10% CO_2 and 10% O_2 and 0.8 g of catalyst (space time range: 1757-1106 g h mol^{-1}). Temperature of reactor varied between 250 ºC and 500 ºC. Reaction at 500 ºC and 2.7 l_S min^{-1} was performed to provoke higher reaction rates involving more production of heat and a higher mass, and hence heat, transfer. Obtained results are shown in Table 4.3.

Table 4.3. *Temperature difference between the fixed bed's inlet and outlet.*
$\Delta T = T_{inlet} - T_{outlet}$

$T_{Reactor}$, ºC	250	300	400	500
Q, l_S min^{-1}	1.7	1.7	1.7	2.7
ΔT_{inert}, ºC	0.00	0.85	1.69	0.00
$\Delta T_{reaction}$, ºC	0.13	-0.32	1.69	1.74

Similar results were obtained for different reaction conditions. Observed differences between the two points' temperatures once steady state was reached were no higher than 2 ºC while the catalyst was being dried with the Ar flow or when reaction was occurring. Because of that temperature differences were attributed to experimental error of the measurement system and it was concluded that gradients in the reactor were negligible, so a isothermal reactor was considered.

4.2.2 Theoretical results

Data obtained from experimentation was used to ensure theoretically that the observed reaction rate is not affected by diffusion stages. Data from reactions in limit conditions was used for the calculations, with lowest performable flow rate and highest sieved catalyst particles: 1.5 l_S min^{-1} and 0.2 mm.

4.2.2.1 External diffusion

External diffusion was judged theoretically by Mear's criterion (Equation (14)), as mentioned in section 3.4.1.1.

$$\frac{(-r_A)_{obs}\ \rho_L\ r_P\ n}{k_c\ C_{A0}} < 0.15 \qquad (14)$$

Reaction data obtained in limit space time (311 g h mol_{NO}^{-1} and 933 g h $mol_{o\text{-}DCB}^{-1}$) was used to evaluate the compliance of the criterion. This way, any better condition (further from the limit) would ensure absence of mass-transfer's effect. Data is summarised in Table 4.4.

Reaction rate in heterogeneous catalysis is defined as:

$$-r_A = \frac{dx_A}{d(W/F_{A0})} \quad (20)$$

For low conversions in a differential reactor Equation (20) can be simplified to:

$$-r_A \approx \frac{x_A}{W/F_{A0}} \quad (21)$$

Although the reaction system could not be considered differential, the reaction rates were calculated with this approximation in order to get a result. Limit reaction rates obtained this way were 2.0 10^{-3} mol h^{-1} g^{-1} for NO at 200 ºC and 2.9 10^{-4} mol h^{-1} g^{-1} for o-DCB at 250 ºC.

Mass transfer coefficient was calculated by Ranz-Marshall correlation (Green and Perry, 2008):

$$Sh = 2 + 0.6\, Re^{0.5}\, Sc^{\frac{1}{3}} \quad (22)$$

Where Sherwood's dimensionless number is:

$$Sh = \frac{k_C\, d_P}{D_{AB}} \quad (23)$$

And Schmidt's and Reynolds' dimensionless numbers were obtained by:

$$Sc = \frac{\mu}{\rho_A\, D_{AB}} \quad (24)$$

$$Re = \frac{u\, d_P\, \rho_A}{\mu_A} \quad (25)$$

Where gas mixture's density and viscosity were supposed to be as a exclusively argon's and ideal behaviour was considered.

Diffusion of reactants in Ar, considering a binary mixture for each reagent, was obtained by the equation of Fuller-Schettler-Giddings (Vielstich, et al. 2003):

$$D_{AB} = \frac{10^{-3}\, T^{1.75} \left(\frac{1}{M_A} + \frac{1}{M_B}\right)^{0.5}}{P\left[(\Sigma V_m)_A^{\frac{1}{3}} + (\Sigma V_m)_B^{\frac{1}{3}} \right]^2} \quad (26)$$

Table 4.4. *Summary of Equation (14) parameters' values.*

Parameter	Value	
	NO	o-DCB
$(-r_A)$, mol h^{-1} g^{-1}	$2.0\ 10^{-3}$	$2.90\ 10^{-4}$
C_A, mol m^{-3}	$1.16\ 10^{-2}$	$3.49\ 10^{-3}$
ρ_L, kg m^{-3}	1000	
r_P, m	0.1	
n	1	
ρ_{Ar}, kg m^{-3}	1.40	
μ_{Ar}, kg m^{-1} s^{-1}	$3.54\ 10^{-5}$	
Re	2.37	
k_C, m s^{-1}	0.47	0.19
Sc	0.67	2.11
Sh	2.81	3.19
V_m (Ar), cm^3 mol^{-1}	16.1	
V_m, cm^3 mol^{-1}	11.17	125.72
D_{AB}, m^2 s^{-1}	$3.41\ 10^{-5}$	$1.20\ 10^{-5}$

Results of Equation (14) were: $1.31\ 10^{-2} << 0.15$ for NO and $1.27\ 10^{-2} << 0.15$ for o-DCB. Therefore, external diffusion's effect was corroborated to be negligible, confirming experimental results theoretically.

4.2.2.2 Internal diffusion

Internal diffusion was evaluated by Weisz-Prater criterion, Equation (16), section 3.4.1.1.

$$\frac{(-r_A)_{obs}\ \rho_C\ r_P^{\,2}}{D_E\ C_A} < 1 \qquad (16)$$

Same experimental data as in the external diffusion (section 4.2.2.1) was used to test the compliance of the criterion.

Density of catalyst was required this time, which was calculated by the combination of the support's density and the volume of pore resulted from the adsorption of N_2:

$$\rho_C = \frac{1}{\frac{1}{\rho_S} + V_P} \qquad (27)$$

Effective diffusion coefficient was calculated theoretically as a function function of Knudsen's diffusivity (diffusion that occurs in the pore), binary diffusivity of reactants in Ar, catalyst particles porosity and tortuosity (Green and Perry, 2008):

$$D_E = \frac{\varepsilon_C}{\tau_C \left(\frac{1}{D_{AB}} + \frac{1}{D_K}\right)} \qquad (28)$$

Catalyst particles porosity was calculated by the relation between the catalyst's density and the volume of pore (González-Velasco, et al. 1999):

$$\varepsilon_C = V_P \, \rho_C \qquad (29)$$

Tortuosity in a particle was difficult to calculate so it was estimated as the inverse of the porosity:

$$\tau_C = \frac{1}{\varepsilon_C} \qquad (30)$$

Knudsen's diffusivity needed to be considered to take into account the diffusion that happens inside the catalyst's pores. It was calculated with the following formula:

$$D_K = 48.5 \, d_{pore} \sqrt{\frac{T}{M_A}} \qquad (31)$$

Moreover, the effective diffusion coefficient was also calculated experimentally due to the complexity of the gas mixture. This was carried out by the comparison of the reaction rate under internal diffusion control and without it (Both cases are shown in Figure 4.4 B). That efficiency factor (The relation between the conversions) led to a calculable Thiele modulus by the following expression:

$$\eta = \left(\frac{\phi}{\tanh(\phi)} - 1 \right) \frac{3}{\phi^2} \qquad (32)$$

The experimental effective diffusivity was estimated by:

$$D_E = \frac{(-r_A) \, \rho_C \, r_P^{\,2}}{C_A \, \phi^2} \qquad (33)$$

Used reaction data is summarised in Table 4.5.

Effective diffusivity values happened to be so different depending on the estimation method, being experimentally calculated diffusivity 5 times higher for NO and 9 for o-DCB than estimated. Because of that difference, experimental values were taken into account for the acceptance of the non-existence of internal diffusion's effect. The results of Equation (16) were: $0.34 < 1$ for NO and $0.20 < 1$ for o-DCB.

Table 4.5. *Summary of data for external diffusion analysis. Data in italics was obtained from 0.65 average diameter catalyst particles, under diffusion control.*

Parameter	Value		
	NO		o-DCB
$(-r_A)$, mol h^{-1} g^{-1}	$2.0\ 10^{-3}$		$2.90\ 10^{-4}$
C_A, mol m^{-3}	$1.16\ 10^{-2}$		$3.49\ 10^{-3}$
ρ_C, kg m^{-3}		2027	
r_P, m		0.1	
V_P, m^3 kg^{-1}		$2.3\ 10^{-4}$	
ε		0.47	
τ		2.14	
D_K, m^2 s^{-1}	$2.89\ 10^{-6}$		$1.35\ 10^{-6}$
D_{AB}, m^2 s^{-1}	$3.41\ 10^{-5}$		$1.20\ 10^{-5}$
$D_{E\ Theo}$, m^2 s^{-1}	$5.79\ 10^{-7}$		$2.63\ 10^{-7}$
r_P, m		*0.33*	
$(-r_A)_{obs}$, mol h^{-1} g^{-1}	*$1.69\ 10^{-4}$*		*$2.60\ 10^{-4}$*
η	*0.85*		*0.90*
ϕ	*1.71*		*1.35*
$D_{E\ Exp}$, m^2 s^{-1}	*$2.96\ 10^{-6}$*		*$2.43\ 10^{-6}$*

The compliance of the criterion for the internal diffusion was not as clear as the one for the external. That could be predicted from the experimental results since while there was not observed any difference in the conversion with different flow rates, there was observed a difference between the biggest and smalles particles. That implies that internal diffusion is closer to the borderline of being the limiter stage than the external. Nevertheless, it was considered sufficient to conclude that the system was free of internal diffusion's effect.

4.2.2.3 Heat transmission

A heat balance was performed for a catalyst particle, to estimate which would be the temperature gradient caused by the reaction heat between the particle surface and the flow. o-DCB's total oxidations reaction heat has been taken into account for being much higher than NO's selective reduction's: -407.07 kJ mol_{NO}^{-1} and -2448.25 kJ $mol_{o\text{-}DCB}^{-1}$.

Reaction heat was transformed to convective heat flow:

$$Q_C = \Delta H\ (-r_A)\ w_P = \Delta H\ (-r_A)\ \rho_C\ \frac{4\ \pi\ r_P^{\,3}}{3} \qquad (34)$$

If a full forced convective heat-flow is assumed:

$$Q_C = A\ h_C\ \Delta T \qquad (35)$$

Convective heat transmission coefficient for Equation (35) has been estimated though the dimensionless number of Nusselt, which depends on the Reynolds' (Equation (25)) and

Prantdl's dimensionless numbers, which is recommended by Whitaker in (Green and Perry, 2008) for isothermal spherical particles in forced convection.

$$Nu = 2 + \left(0.4\, Re^{\frac{1}{2}} + 0.06\, Re^{\frac{2}{3}} \right) Pr^{0.4} \left(\frac{\mu_{\infty}}{\mu_S} \right)^{\frac{1}{4}} \quad (36)$$

Where,

$$Pr = \frac{C_p\, \mu_A}{k} \quad (37)$$

Values obtained are summarised in Table 4.6.

Table 4.6. *Calculations summary for estimation of convective heat transfer coefficient.*

Parameter	Value
d_P, mm	0.2
w_P, kg	$8.49\ 10^{-9}$
$(-r_A)$, mol $kg^{-1}\ s^{-1}$	$8.04\ 10^{-5}$
Q_C, J s^{-1}	$-1.67\ 10^{-9}$
A, m^2	$1.26\ 10^{-7}$
k_{Ar}, J $s^{-1}\ m^{-1}\ ºC^{-1}$	0.018
Re	2.37
C_P, J $kg^{-1}\ ºC^{-1}$	519.38
μ_{Ar}, kg $m^{-1}\ s^{-1}$	$3.54\ 10^{-5}$
Pr	1.02
Nu	2.73

Nusselt's dimensionless number is the relation between the heat transfer that occurs by convection and the heat transfer that occurs by conduction:

$$Nu = \frac{h_C\, d_P}{k_C} \quad (38)$$

Solving Equation (38) a convective heat transfer coefficient of 245.59 W $m^{-2}\ ºC^{-1}$ was obtained. That value, led to a temperature gradient of $5.42\ 10^{-4}$ ºC solving Equation (35), which was considered to be negligible.

4.3 POTENTIAL KINETICS

In order to get a empirical expression for the reaction rate, reactions were performed simultaneously (nominal feed composition, Table 3.1) at different space time values and temperatures, above the limit conditions defined in the previous 4.2.1.1 section. Space time was changed varying the volumetric flow rate (1.5 $l_S\ min^{-1}$ - 2.5 $l_S\ min^{-1}$) and the catalyst mass (0.5 g - 1.5 g). Obtained results are shown in Figure 4.6.

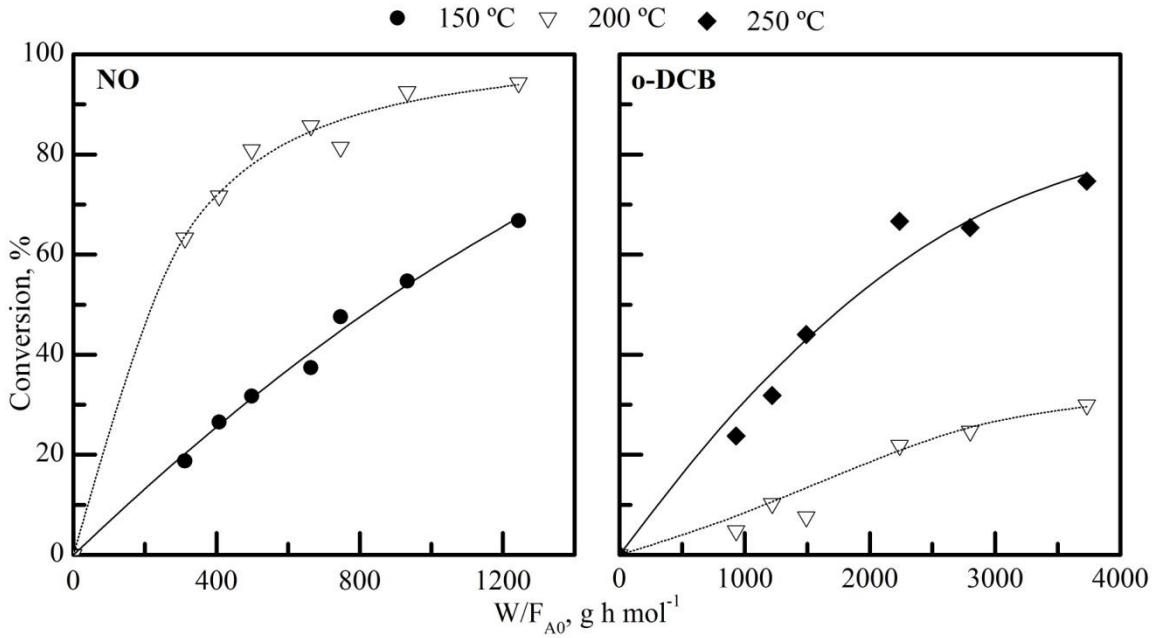

Figure 4.6. *Effect of space time in reagents' conversions at different temperatures.*

As expected, an increase on both pollutants conversion was observed by enlarging space time.

Conversion vs. space time curves usually adjust well to quadratic equations. Because of that, experimental data obtained at temperatures in which a wide range of conversions was observed in the tested space times (150 ºC for NO and 250 ºC for o-DCB) was adjusted to those equations. The obtained equations were:

$$x_{NO,\,150\,^{o}C} = -1.17\ 10^{-7}\left(\frac{W}{F_{0,\,NO}}\right)^{2} + 6.87\ 10^{-4}\left(\frac{W}{F_{0,\,NO}}\right) \qquad (39)$$

$$x_{o\text{-}DCB,\,250\,^{o}C} = -3.75\ 10^{-8}\left(\frac{W}{F_{0,\,o\text{-}DCB}}\right)^{2} + 3.44\ 10^{-4}\left(\frac{W}{F_{0,\,o\text{-}DCB}}\right) \qquad (40)$$

Derivation of Equations (39) and (40) gave the value of reaction rate applying Equation (20). This way, reaction rate was given by the following expressions:

$$(-r_{NO})_{150\,^{o}C} = -2.34\ 10^{-7}\left(\frac{W}{F_{0,\,NO}}\right) + 6.87\ 10^{-4} \qquad (41)$$

$$(-r_{o\text{-}DCB})_{250\,^{o}C} = -7.5\ 10^{-8}\left(\frac{W}{F_{0,\,o\text{-}DCB}}\right) + 3.44\ 10^{-4} \qquad (42)$$

Where space time is introduced in g h mol^{-1} unit and reaction rate is given in mol g^{-1} h^{-1}.

These reaction rates describe the experimental behaviour of each of the reactions happening simultaneously. Afterwards it will be proved that there are interactions between both reactions.

Besides that, it is reported in literature that both reactions are of first order rate law kinetics. Because of that experimental data has been adjusted to simple first order potential equation.

Reaction rate in a first-order reaction is given by the following expression:

$$(-r_A) = k' C_A = k' C_{A0} (1 - x_A) \quad (43)$$

Which can be equalized in this case to the reaction rate expression in heterogeneous catalysis in Equation (20):

$$\frac{dx_A}{d\left(\frac{W}{F_{A0}}\right)} = k' C_{A0} (1 - x_A) \quad (44)$$

And this can be integrated:

$$\int_0^{x_A} \frac{dx_A}{(1-x_A)} = k' C_{A0} \frac{W}{F_{A0}} \quad (45)$$

Giving the following solution:

$$-\ln(1 - x_A) = k' C_{A0} \frac{W}{F_{A0}} \quad (46)$$

Equation (46) is a linear function. Experimental results were adjusted to a *-ln(x_A) vs. W/F_{A0}* line in Figure 4.7.

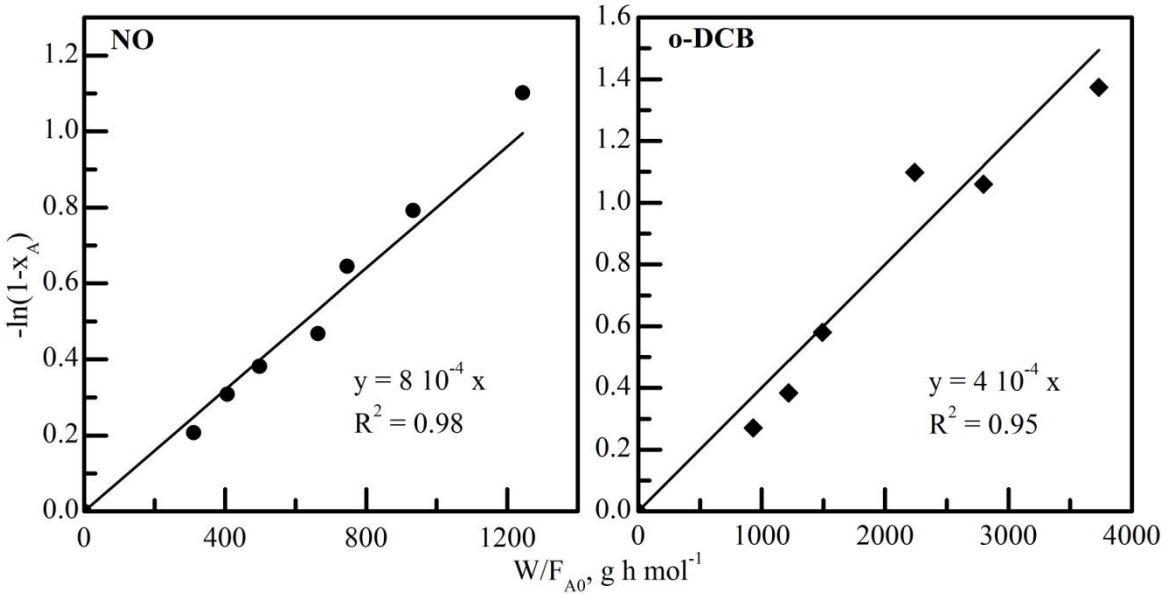

Figure 4.7. *Linear expression of first order reaction.*

It was proved that, as previously was reported, reactions are of first order for NO (Busca, et al. 1998) and o-DCB (Wielgosinski, et al. 2007; Krishnamoorthy, et al. 1998; Stoll et al. 2001) since experimental data could be acceptably fitted the linear Equation (46) with

deviations of 7.4% for NO and 12.2% for o-DCB. The residuals of the estimation are shown in Figure 4.8. As a proof of the good quality of the regression it is observed that experimental data is dispersed randomly close to the regression.

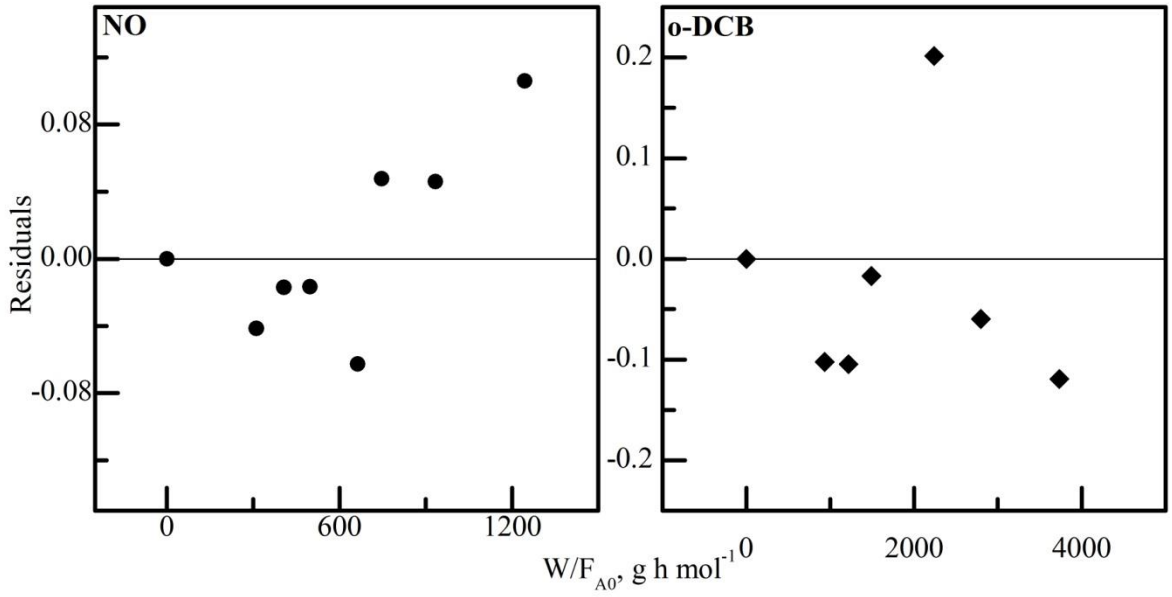

Figure 4.8. *Resilduals for first order's linear regression.*

Lines' slopes in Figure 4.7 correspond to term k C_{A0}, substituting initial concentrations' values (1.3 10^{-2} mol_{NO} m^{-3} and 3.5 10^{-3} $mol_{o\text{-}DCB}$ m^{-3}), the following kinetic constants were obtained:

$$k'_{NO,\ 150\ ^{o}C} = 0.062 \pm 4\ 10^{-3}\ m^3\ g^{-1}\ h^{-1}$$

$$k'_{o\text{-}DCB,\ 250\ ^{o}C} = 0.115 \pm 0.013\ m^3\ g^{-1}\ h^{-1}$$

4.4 MECANISTIC KINETICS

The objective of this section is to propose the mechanistic reaction rate equation. Therefore, firstly differences between the combined and independent reactions were analyzed and then the effect of the different reactants' concentrations.

4.4.1 Simultaneous reaction vs. individual reactions

A preliminary study was carried out to view the influence or effect of the SCR reaction on the CTO reaction and vice-versa. To carry out the study, initially nominal conditions (Table 3.1) were established for reactions and once steady state was reached, NH_3 and NO were eliminated from the feed stream to study the effect on the conversion of o-DCB. The same procedure was repeated the other way around, o-DCB was eliminated from the complete feed stream to analyze the effect on the conversion of NO. Reactions were performed at different temperatures as it is shown in Figure 4.9.

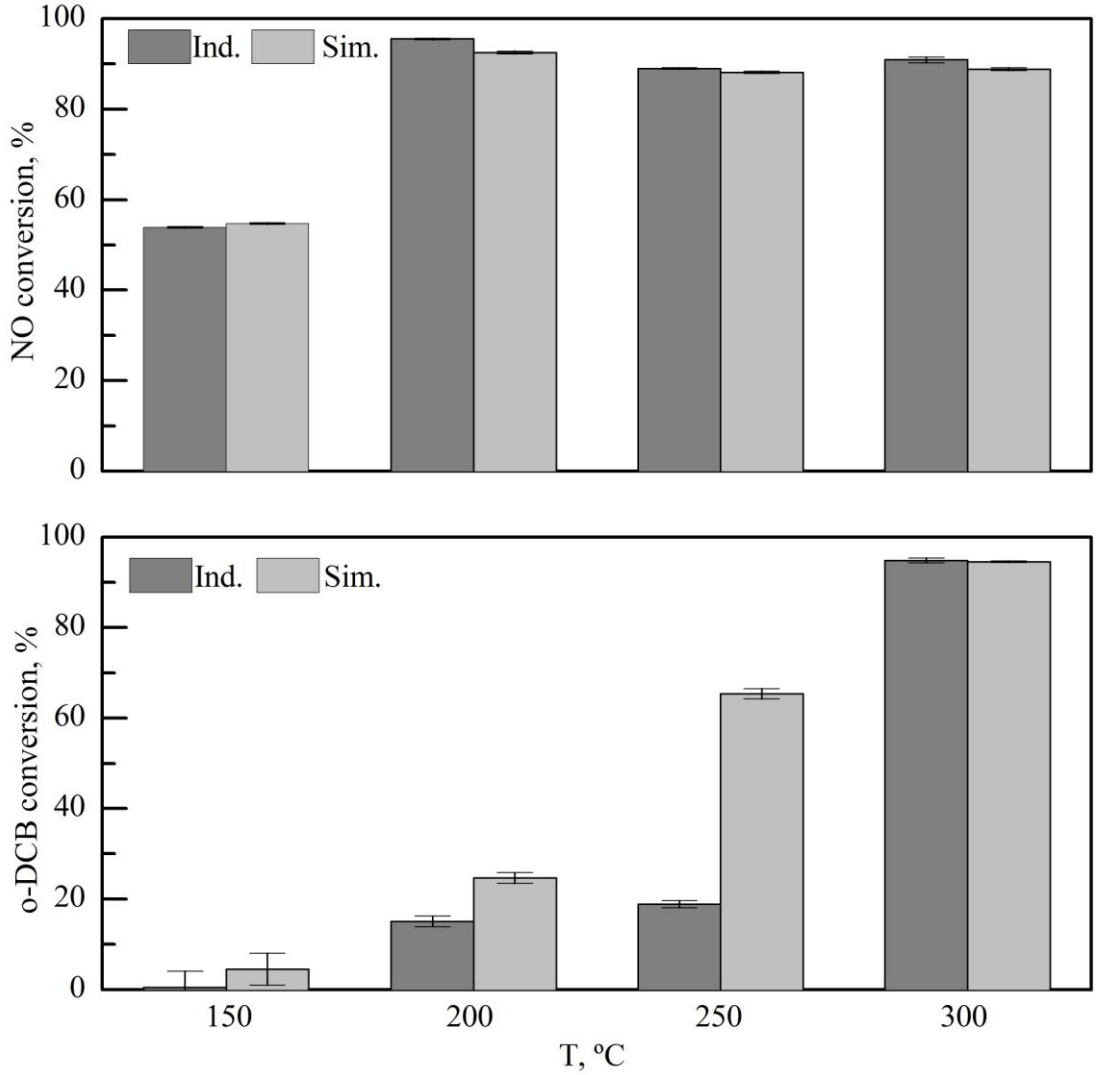

Figure 4.9. *Preliminary reactions to view effect of one reaction on the other. Performance with 1.5 g and 2 l_S min^{-1} at space times of 933 h g^{-1} mol_{NO}^{-1} and 2800 h g^{-1} $mol_{o\text{-}DCB}^{-1}$.*

A little difference between the independent and the simultaneous reaction was observed in the decomposition of NO. On one hand, at 150 ºC there was a slight enhance of the 1.4% in the NO conversion when o-DCB was co-fed, which could be disdained since the deviation of that are nearly overlapped and has been previously reported within the experimental error of the equipment (Gallastegi-Villa, et al. 2015). On the other hand, in the rest of the temperature range the o-DCB had a negative effect, with a deterioration of more than the 2.5%. In contrast, the efficiency of the abatement of o-DCB showed a prominent improvement when NO and NH_3 were co-fed in all of the tested temperatures, despite the effect was too low at 300 ºC.

In SCR of NO, the first step is the adsorption of ammonia in an acidic site followed by an activation of it via redox reaction reducing the adjacent V^{5+} to V^{4+}. Then, the activated complex react with NO which can be in the gas phase or weakly adsorbed, taking place the SCR reaction. Finally, the reoxidation of the vanadia site takes place closing the redox cycle (Busca, et al. 1998). Otherwise, there is not a fixed agreement on the reaction mechanism of

o-DCB's CTO. Wang, et al. (2015) reported that a chlorobenzene molecule is adsorbed in an acidic site by the substitution of a C-Cl bond, being the chlorine atom attached to the vanadium in the acidic site and the benzene bonded with a oxygen-bridge bond. In this regard, Gallastegi-Villa, et al. (2015) reported that monomeric vanadia sites were more active for abatement of o-DCB and polymeric for NO, but that both species were active in both reactions.

Taking into account the mentioned mechanism theories, and also others, a competition for the acidic sites would be expected. This competition would explain the worsening of the NO conversion in presence of o-DCB. That competition was proved by Gallastegi-Villa, et al. (2015) by feeding ammonia in excess where a notorious decrease on the conversion of o-DCB was observed. Moreover, same results are reported in the next section 4.4.2.

Additionally, presence of HCl (produced from oxidation of o-DCB) could react with NH_3 and led to the formation of NH_4Cl (Equation (9)). In that case, the fed ratio of NO:NH_3 would be lost, with the subsequent decay of the SCR's effectiveness. In this sense, Hou, et al. (2014) reported that presence of NH_4Cl can act as poison for the catalyst but also as a promoter by increasing the acidity of the surface. The slight improvement of performance in the simultaneous reaction at 150 ºC (Figure 4.9) could be due to this, since formation of NH_4Cl salt more likely to precipitate on the catalyst at lower temperatures. It is noteworthy that the appearance of this salt was observed in the reactor outlet stream, in the sections were the tubes were not heated, when o-DCB and NH_3 were fed.

In case of o-DCB's oxidation, an increase of conversion was observed at 200 ºC (63.6%) and 250 ºC (246.8%). The enhancement of the conversion of o-DCB in presence of NH_3 and NO could be due to the formation of NO_2 which has a higher oxidation potential than oxygen. Then, NO_2 could participate in the oxidation reaction of o-DCB assisting or at least partially replacing O_2 to recover the V^{5+} species and close the redox cycle. A similar behaviour was observed by Bertinchamps, et al. (2005) who observed that chlorobenzene conversion increased from 45,5 to 69,5% with $VO_X/WO_3/TiO_2$ catalyst by addition of 100 ppm of NO. Moreover, recently Su, et al. (2015) also reported that NO has a positive effect on the degradation of 1,2,4-triclorobence. They got a conversion of the 51-60% of 1,2,4-triclorobence over $Ce_{0.2}TiAl_{0.2}O_X$ and $Ce_{0.2}TiO_X$ catalyst in absence of NO that increased to 73-87% by NO addition. Additionally, the positive effect of NO in the abatement of pentachlorobenzene was reported by Xu, et al. (2012).

The positive effect of the simultaneous feeding in the conversion of o-DCB decreased at 300 ºC because of lack of NO_2. NO_2 and NO are gases in equilibrium, which is shifted towards NO_2 in low temperatures and towards NO in higher ones. Because of that, NO_X mixture is mostly NO at 300 ºC and the only oxidation agent is O_2. A similar behaviour was previously reported by Xue, et al. (2013) who studied the conversion of chlorobenzene in presence of NO over V_2O_5/TiO_2 catalyst. In addition, the competitive mechanism between both reactions mentioned above became more evident at high temperatures.

4.4.2 Feed's composition's effect in reactions

Reactants concentration in feed stream was modified to study the effect in conversion and selectivity in order to obtain the mechanistic kinetic model.

In order to obtain a whole kinetic model for the reaction feed's composition would have to be changed in different temperatures, since different interactions between reactions were observed in the previous 4.4.1 section depending on the temperature (Figure 4.9). Unfortunately, because of system's complexity, experimental difficulties and timing limitations, the study was performed at two temperatures. On one hand, the SCR was evaluated at 150 ºC, where conversion of nearly the half of the fed NO was converted. In this regard, conversion of NO and selectivity towards N_2O were calculated in reactions at the given temperature. On the other hand, the o-DCB's CTO reaction was studied at 250 ºC. At that temperature effect of the presence of NO and NH_3 in the reaction was big and conversion values' standard deviation was low enough to assure a good level of accuracy. Selectivity towards CO and CO_2 and conversion of o-DCB were measured in reactions performed at 250 ºC.

Influence of CO_2

Monitoring carbon dioxide's concentration in the reaction outlet is interesting to measure in order to obtain o-DCB's oxidation's selectivity values towards CO and CO_2. Up to now, CO_2 was co-fed with the reagents (Table 3.1) in order to simulate as best the real MWI plant's combustion gases. At most 600 ppm of CO_2 (100% selectivity) could be formed feeding the nominal 100 ppm of o-DCB. In this regard, the employed analysis system was not able to measure this small differences in the measure range of 0 - 10% (vol.) that the analyzer was calibrated to measure in order to monitor the fed concentration. Because of that, the effect of CO_2 in the conversion of o-DCB and NO was checked by analyzing the difference between the conversions obtained in presence of CO_2 and the ones obtained in absence.

Reaction was performed at the same conditions (250 ºC, 933 h g^{-1} mol_{NO}^{-1} and 2800 h g^{-1} $mol_{o\text{-}DCB}^{-1}$) in absence and presence of 10% (vol.) of CO_2, and nominal concentrations (Table 3.1) of the rest of reactants. There was observed no difference between one reaction and the other, conversion values of 92% NO and 67% o-DCB. The absence of effect of CO_2 in the CTO of o-DCB has also been previously reported by Stoll, et al. (2001).

The following reactions were performed with the nominal feed (Table 3.1) without CO_2, using 1.5 g of catalyst at a volumetric flow rate of 2 l_S min^{-1}. The modification of flow rate for each reactant was balanced with inert Ar.

4.4.2.1 Influence of o-DCB

Influence of o-DCB in the reaction was measured by carrying out reaction feeding 60, 100 and 250 ppm concentrations. The highest concentration was set in order to comply the limit space time established in the previous section 4.2.1.1. Results of conversion of NO from the reaction performed without o-DCB are also shown for comparison. Effect of o-DCB is shown in Figure 4.10. Standard deviation of conversion of o-DCB is only shown since the rest of parameters did not vary significantly and representation of the deviation did not contribute at all.

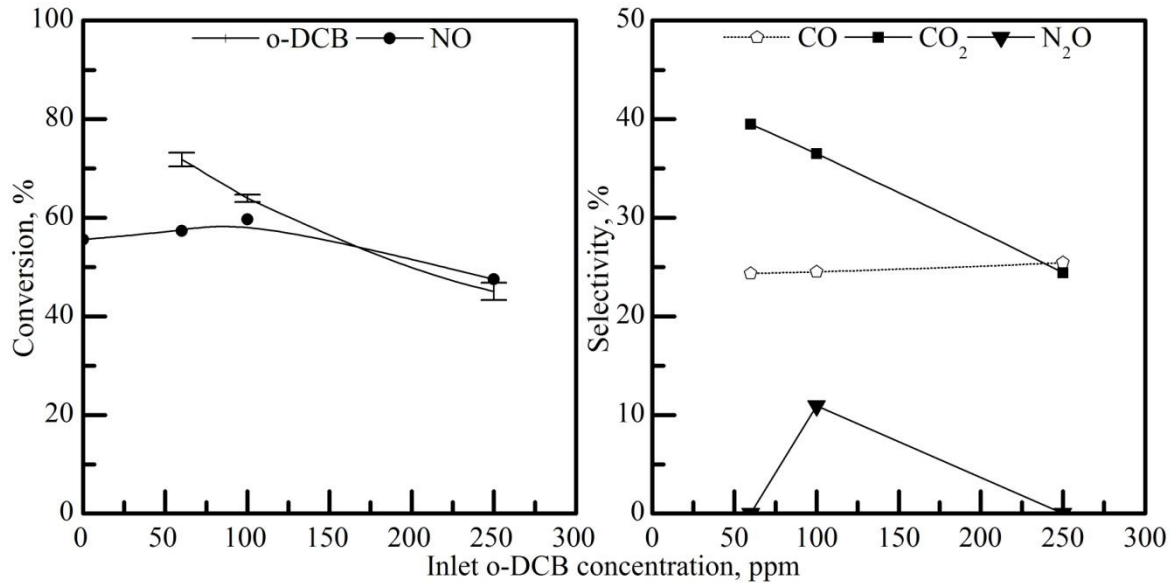

Figure 4.10. *Effect of o-DCB concentration in conversion and selectivity.*

It was observed that conversion of o-DCB decreased inversely proportional to the fed o-DCB. That tendency would confirm a first order reaction if a differential reactor was estimated (Krishnamoorthy, et al. 1998). NO's conversion level did not change significantly in the tested concentrations. However, a slight decrease of conversion could be appreciated when 250 ppm of o-DCB were fed. This decrease was considered to happen due to a higher formation rate of HCl (and so NH_4Cl) or because of competition between NH_3 and o-DCB for catalyst's acidic sites as mentioned before.

Selectivity towards CO increased slightly with the increase of o-DCB in the feed-stream. On the contrary, selectivity towards CO_2 decreased considerably. It is noteworthy that carbon balance was not closed (60% of introduced was quantified at most), so other unquantified reaction products were formed, which were identified by chromatography: Maleic anhydre and dichloromaleic anhydre. The formation of these compounds has been previously reported by (Albonetti, et al. 2008).

On its behalf, the selectivity towards N_2O did not show a conclusive tendency. Moreover, it was too low (below 10%) so the difference was rejected.

4.4.2.2 Influence of NO-NH_3

Feeding of the SCR was modified keeping the nominal 1.13:1 molar ratio of NH_3:NO and modifying concentration of NO: 150 ppm, 300 ppm and 830 ppm. The highest concentration was set in order to comply the limit space time established in the previous section 4.2.1.1. Results of conversion of o-DCB without feeding NO-NH_3 are also shown together with the rest of the results in Figure 4.11.

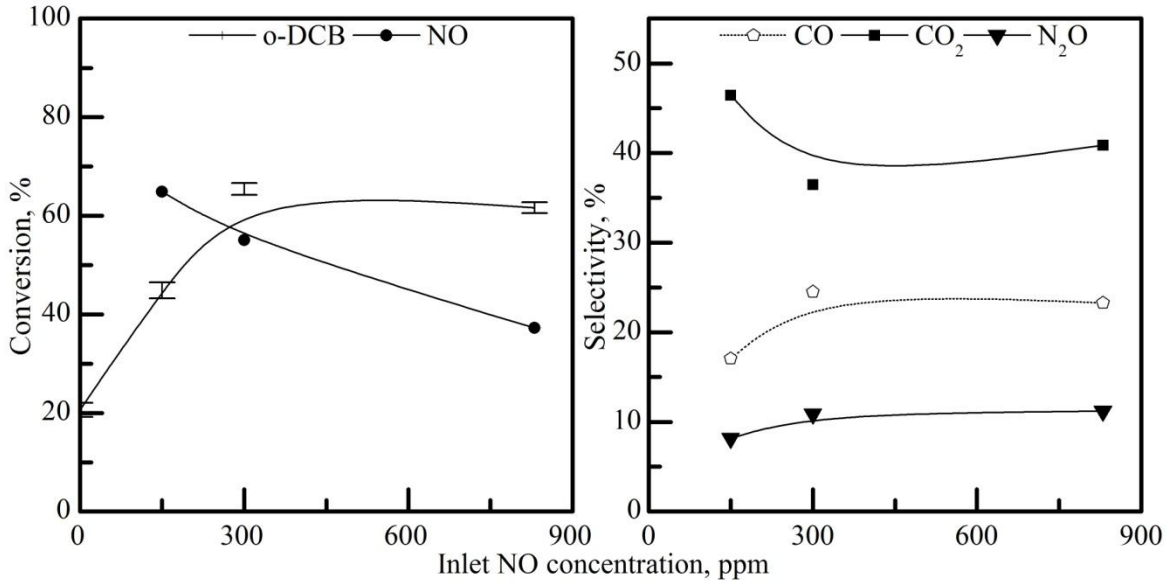

Figure 4.11. *Effect of NO-NH_3 concentration in conversion and selectivity.*

A decrease of NO conversion was observed when higher concentrations were fed to reactor. As it is mentioned previously this tendency fits to first order potential reaction if the reaction rate is estimated considering a differential reactor.

On the other hand, conversion of o-DCB was enhanced with the addition of NO and NH_3 to the reactor inlet between 0-300 ppm. That behaviour is in line with the previously reported in section 4.4.1. Improvement of catalytic performance could be justified by the presence of NO_2. Then again, when 830 ppm of NO and NH_3 were fed no change was observed. That could be because the competition of NH_3 and o-DCB to be adsorbed in the acidic sites is becoming more evident.

Regarding to selectivity, decomposition of NO to N_2O did not show any change. On the other hand, selectivity of the CTO towards CO slightly increased at higher NO-NH_3 concentrations. Selectivity towards CO_2 did change but it did not follow a tendency, always remaining around 40%. More carbonic products were also assumed since carbon balance was not closed.

4.4.2.3 Influence of the ratio NH_3:NO

Influence of NO and NH_3 concentration relation was measured modifying the fed ammonia concentration with constant NO concentration at 300 ppm. Ammonia was fed in 240, 400 and 570 ppm, getting NH_3:NO molar ratios of sub-stoichiometric feeding (0.8), nominal feeding (1.13) and super-stoichiometric feeding (1.9). Tests results are shown in Figure 4.12.

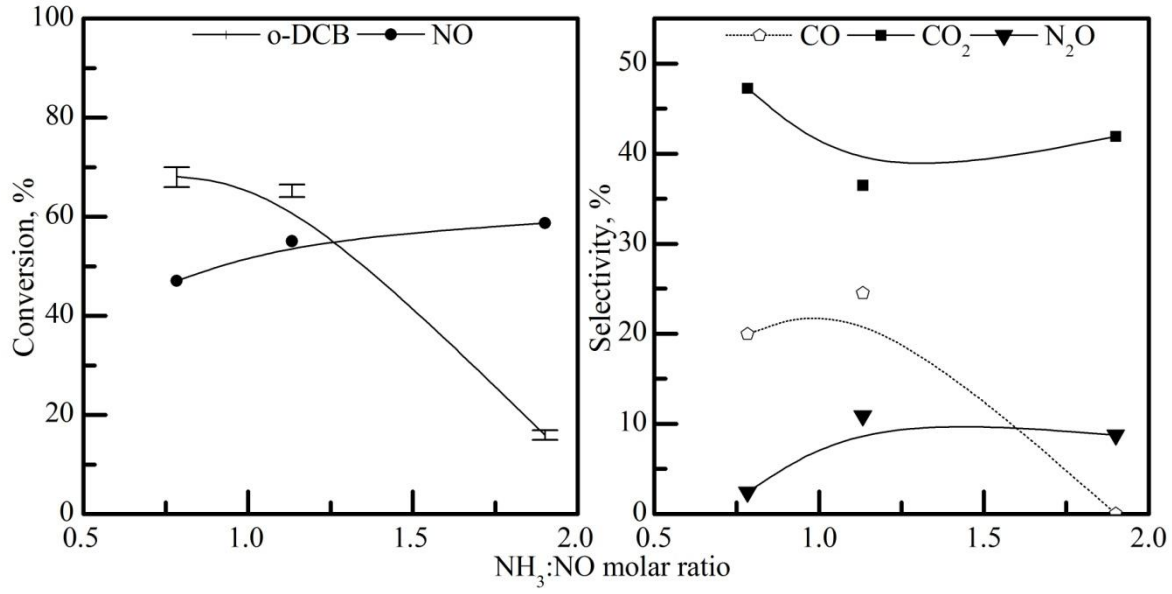

Figure 4.12. *Effect of NH_3:NO ratio in conversion and selectivity.*

Abatement of NO was enhanced by feeding of excess of ammonia. To contrary, conversion of o-DCB decreased slightly. This facts, together with the results of the previous section confirm that positive (NO) and negative (NH_3) effects coexist in the combined abatement of o-DCB with NO. The same effects of NO and NH_3 were previously reported by Xue, et al. (2013) in the chlorobezene's catalytic oxidation over V_2O_5/TiO_2.

At low ammonia ratio o-DCB's conversion was slightly improved and NO's decreased. This is in line with the mentioned effects, since with lower ammonia concentrations lower SCR reaction rates would be observed and more NO would be available to be oxidized to NO_2 and consequently improve o-DCB's oxidation. Bertinchamps, et al. (2005) concluded the same effect feeding only NO to the oxidation of o-DCB. Additionally, at lower ammonia ratio the probability of the possible competition between the o-DCB and NH_3 to adsorb in acid sites is also reduced.

This results are in good agreement with Xu, et al. (2012) work, where NO and NH_3 effects were studied in the oxidation of pentachlorobenzene. They reported a gradual enhance of pentachlorobenzene's abatement by changing concentration of only NO from 0 to 1000 ppm. Furhtermore, the addition of NO until 2000 ppm did not affect the conversion level.

In terms of selectivity, it is remarkable that when excess of ammonia was fed, conversion of o-DCB towards CO was 0. Selectivity towards CO_2 did not exhibit any tendency. The abatement of NO gave lower selectivity towards N_2O with a defect of ammonia feeding what implies that the SCR towards N_2 is enhanced in this conditions.

4.4.2.4 Influence of O_2

Oxygen, which was nominally fed in excess in order to imitate the real situation in the flue gas of a MWI, was studied at less concentration and also catalytic tests were carried out with no oxygen. Results of catalytic tests carried out in such conditions are shown in Figure 4.13.

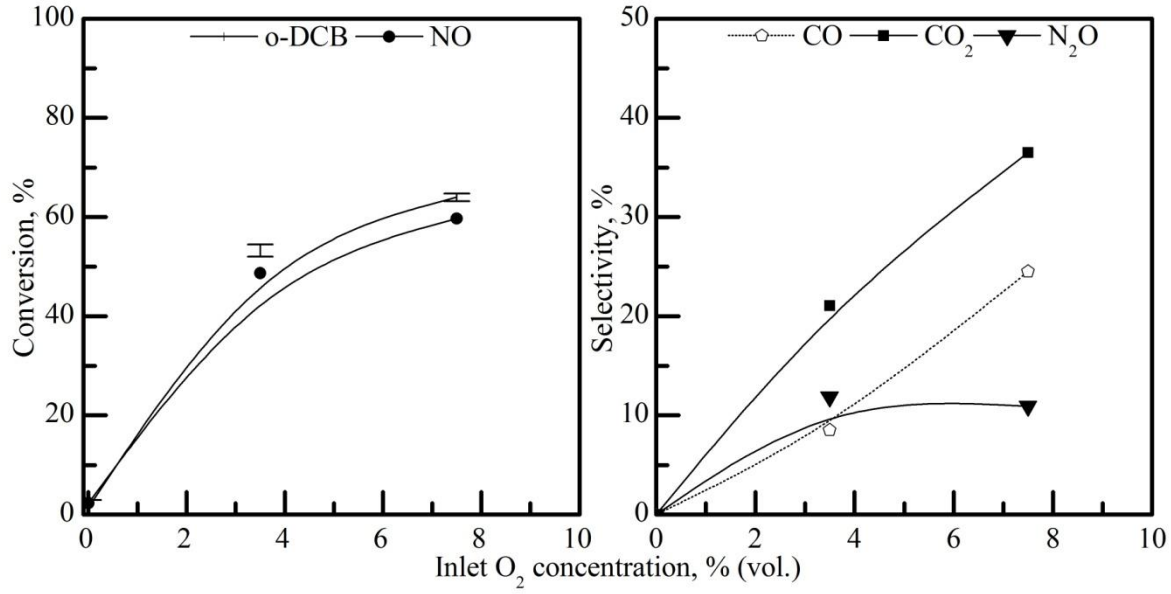

Figure 4.13. *Effect of O_2 in conversion and selectivity.*

Both reactions showed a big dependence on the availability of oxygen. As expected no conversion was observed neither for o-DCB nor NO with lack of oxygen. In presence of oxygen, both reactions showed an improved behaviour, the more oxygen was fed the higher abatement was achieved. A similar behaviour was previously reported for o-DCB (Stoll, et al. 2001) and monochlorobenzene (Bertinchamps, et al. 2005; Stoll, et al. 2001).

Regarding to selectivity, less N_2O was formed with higher oxygen concentrations, implying a more selective (towards N_2) abatement of NO by SCR reaction. Selectivity towards CO and CO_2 increased with the addition of oxygen, which involves an enhanced oxidation of o-DCB rather than conversion to side-products.

4.4.3 Mechanistic reaction rate expression

Mechanistic reaction rate equations are obtained by taking into account the chemical adsorption and desorption of reactants and products. Different reaction mechanisms involve different mathematical expressions, much more complex than the potential equations.

The most used kinetic mechanisms are shown in Figure 4.14: the Langmuir-Hinshelwood (LH), the Eley-Rideal (ER) and Mars-Van-Krevelen (MVK). The LH mechanism describes the surface catalytic reaction between two adsorbed reagents. On the other hand, the ER mechanism proposes a chemical reaction of an adsorbed (1) compound with a compound in gas phase (2), directly, without adsorbing. In the MVK mechanism the surface of the catalyst is an active part, since a reactant layer is chemically bonded to it (1a). The other reactant reacts directly from gas (1b) and the vacancy of the surface appeared after the desorption of the product is filled again by the first reactant.

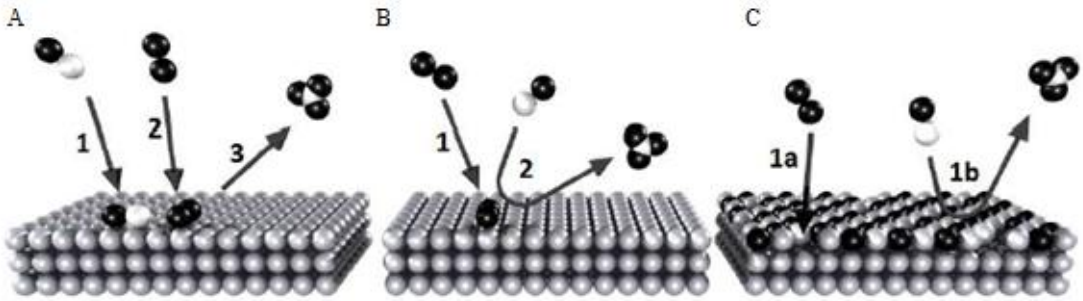

Figure 4.14. *Heterogeneous catalytic reaction mechanisms of Langmuir-Hinshelwood (A), Eley-Rideal (B) and Mars-Van-Krevelen (C).*

All the mentioned mechanistic kinetic equations use to have the following structure:

$$(-r_A) = \frac{(\text{constant})\left(\begin{array}{c}\text{composition, pressure or}\\ \text{equilibrium shift gradient}\end{array}\right)}{(\text{resistance or adsorption})} \qquad (47)$$

$$(-r_A) = \frac{k \prod_{i=\text{reagents}} C_i^{n_i}}{1 + \sum_{i=\text{reagents}} K_i C_i^{N_i} + \sum_{j=\text{products}} K_j C_j^{M_j}} \qquad (48)$$

In the search of a mechanistic reaction rate expression, the effect of the different reactants in the reaction rates of the combined abatement of NO and o-DCB was studied in the previous section 4.4.2. It is looked forward that interactions of the different reactants and side products be described by the mathematical expression. Effects have been evaluated in the previously mentioned temperatures, abatement of NO at 150 ºC and abatement of o-DCB at 250 ºC.

Reaction rates, which are required for mechanistic equations adjustment, for different feed stream's compositions are not easy to calculate, since conversion results over different space times are required. Because of that, it was impossible to adjust the obtained experimental results to equations, but a qualitative description of the real mechanistic equation was carried out with the observed effects of different compounds in the reactions' conversions.

4.4.3.1 Reduction of NO

In the expression of reaction rate, both the NO and NH_3 would be placed in the numerator since they have a positive effect for being the main reagents. Oxygen also showed a beneficial effect on the abatement of NO for being able to oxidize de reduced vanadia sites and also because it is a reagent of the stoichiometric Equation (1). To the contrary, o-DCB showed to be detrimental in the elimination of NO due to the competitiveness with NH_3 for adsorbing in an acidic site and also for being the predecessor of HCl leading to the consumption of ammonia formation of NH_4Cl, so in the reaction-rate equation it must occupy a position on the denominator. However, NH_4Cl also exhibited a positive effect due to its deposition in the catalyst's surface, increasing its acidity.

In conclusion, the reaction rate of abatement of NO will resemble to the following expression:

$$(-r_{NO})^{M}_{150\,^{o}C} \propto \frac{k^{M}_{NO}\, C_{NO}{}^{\alpha}\, C_{NH_3}{}^{\beta}\, C_{O_2}{}^{\gamma}\, C_{o\text{-}DCB}{}^{\delta}}{1+ K_{o\text{-}DCB}\, C_{o\text{-}DCB}{}^{\zeta}} \qquad (49)$$

According to the observed results in section 4.4.2 all exponents will be positive, maintaining the reported effects. Exponent of NO will probably be similar to 1 since the reaction-rate equation was adjusted previously to a first power kinetic equation with high precision (section 4.3). Exponents of NO and NH_3 will probably be higher than the ones of o-DCB and O_2 since a higher increase of activity was observed when their concentration increased in feed stream. Moreover, the exponent of O_2 will be close to 0 since even if without its presence no conversion was observed, the abatement of NO did not change significantly when doubling O_2's concentration at super stiochiometric condition (the real condition in a MWI). Finally, it is noteworthy that effect of o-DCB is more prominent as an obstacle than as a promoter, so it's contribution in the equation will be higher in the denominator.

4.4.3.2 Oxidation reaction of o-DCB

The kinetic equation of the abatement of o-DCB must include o-DCB and O_2 in the numerator side, since they are the unique reactants. By its side, NO was reported has beneficial by the formation of NO_2 so it would also appear in the denominator but it would also be a resistance for being a reactant of the parallel reaction happening in the same catalyst. Oppositely, it was shown that ammonia has competitiveness with o-DCB to be adsorbed in acidic sites, so it would appear in the equation as a resistance but also as a driving force due to the enhancement of catalytic activity because the formation of NH_4Cl.

A reaction rate expression similar to the following is predicted:

$$(-r_{o\text{-}DCB})^{M}_{250\,^{o}C} \propto \frac{k^{M}_{o\text{-}DCB}\, C_{o\text{-}DCB}{}^{\alpha}\, C_{O_2}{}^{\beta}\, C_{NO}{}^{\gamma}\, C_{NH_3}{}^{\delta}}{1+ K_{NH_3} C_{NH_3}{}^{\kappa} + K_{NO} C_{NO}{}^{\zeta}} \qquad (50)$$

Positive exponents are assumed to keep the observed effects. Exponent of o-DCB will be close to 1 for its good adjustment to a first order law kinetic (section 4.3). In addition, exponent of O_2 will be close to 0 since there was not observed a big enhance when the double concentration was fed. Apart from that, it is noteworthy that deposition of NH_4Cl is more likely to happen in low temperatures rather than in high ones, and, because of that, the effect of NH_3 is probably more notorious not as a promoter but as a resistance. Moreover, the resistance that NH_3 gives is much more prominent than the one of NO (which implies a higher contribution in the denominator) since a physical competition for an acidic site is assumed. Additionally, the NO one was reported to contribute more as a promoter than as a resistance.

4.5 FURTHER STUDIES

The presented results were conclusive, but a complete description of the kinetic behaviour of the combined abatement of NO and o-DCB over a VO_X/TiO_2 catalyst was not given. In this section the future procedures that have to be carried out are proposed.

On the one hand, in order to adjust the parameters of the proposed mechanistic reaction rate equations (Equations (49) and (50)) in the previous section (4.4.3) values of reaction rate are required in the different performed conditions. For the achievement of that, reactions have

to be repeated in different space times and the obtain a experimental x_A *vs.* W/F_{A0} curve for each case. That way, by graphical or analytical derivation methods, reaction rate values can be obtained.

On the other hand, results of the present project reported that in the simultaneous removal of NO and o-DCB the effects of the different compounds in each reactions vary depending on temperature. In this regard, in order to accomplish a more extended study, evaluation of catalytic tests at different temperatures is proposed as a future activity, in a temperature range of 150 ºC - 300 ºC.

By carrying out the mentioned work, a full description of the so-called deDiNox process modelled in a catalytic reactor that works with a vanadia catalyst supported on titania would be given.

5 CONCLUSIONS

Incineration of MSW is still a resorted method of abatement. The usage of this technique involves exposure to pollutant gases. In this project it was proved that the simultaneous removal of two of the produced pollutant gases, the NO_X and PCDD/PCDFs, can be carried out in a combined process with beneficial results by the catalytic technology.

It was concluded that using particles of 0.2 mm diameter and higher volumetric flow-rates than 1.5 l_S min^{-1} (in the used temperatures) a reactor free of internal and external mass transfer's effects and heat gradients was obtained. This was checked both experimental and theoretically. It is noteworthy that the theoretical estimation of the effective diffusivity was not considered appropriate due to the complexity of the reaction gas mixture.

All the performed catalytic tests showed that reduction of NO and catalytic oxidation of o-DCB can be carried out simultaneously obtaining beneficial effects. At first sight it has been observed that NO is destructed more efficiently at lower temperatures whereas an effective abatement of o-DCB is obtained at higher temperature. Moreover, simultaneous abatement of both the NO and the o-DCB were conclusively adjusted to first order potential kinetic equations.

Independent and simultaneously performed reactions showed that the effects of one reaction in the other depends strongly on temperature. Due to experimental and timing limitations, effects were only studied in detail at one temperature for each reaction (150 ºC for NO and 250 ºC for o-DCB). Regarding to the different interactions between the two destructive reactions in the employed VO_X/TiO_2 catalyst different effects are reported.

From one side, it was observed that the presence of o-DCB does not significantly affect on the SCR reaction of NO. Nevertheless, it was reported that a competitiveness between ammonia and o-DCB exists for the catalyst's acidic sites. Apart from that, o-DCB's contribution to the formation of NH_4Cl was also confirmed, a salt that acts as a promoter or as a resistance for the SCR reaction.

On the other side, the conversion level of o-DCB was drastically affected by the presence of NO and NH_3 in the reactor. On one hand, addition of NO to reactor leds to formation of NO_2 which has a higher oxidation power than the oxygen. In this sense, it was concluded that not only the CTO of o-DCB is enhanced but also reoxidation of the catalyst's reduced sites. On the other hand, presence of NH_3 in the reactor was concluded to be detrimental for the abatement of o-DCB because of competitiveness for the catalyst's acidic sites. Additionally, feeding o-DCB gives rise to formation of NH_4Cl as mentioned above.

Besides, it was concluded that presence of oxygen in the accomplishment of abatement of NO and o-DCB is crucial since conversion without oxygen is not achieved. Additionally, changes in the feeding of oxygen at excess of concentration did not report significant influence on the conversion of NO nor o-DCB.

The efficiency of the SCR of NO and CTO of o-DCB in the combined reaction can also be measured by selectivity towards the desired products. The reduction of NO is so selective towards to N_2 since no high concentrations of N_2O were reported. Regarding to the selectivity of the CTO of o-DCB, the selectivity towards CO and CO_2 was not that constant. The higher was the conversion in any condition the more selective was the oxidation towards CO_2. It is

worth of mention that selectivity towards CO_2 is always higher than the one towards CO. Nevertheless, a carbon balance shows that other by-products are also formed, maleic anhydre and dichloromaleic anhydre.

By the mentioned conclusions a mechanistic reaction rate equation was proposed. For the calculation and optimization of kinetic parameters (reaction orders, kinetic pre-exponential constant, adsorption constants, ...) additional catalytic tests are required, which have been proposed as further studies. Likewise, it is also proposed to extend the study performed in this project at different temperatures since reactions' behaviour was proved to be different depending on the temperature. This way, a complete kinetic mechanism can be described for the combined elimination of NO and o-DCB using a VO_X/TiO_2 catalyst.

6 NOMENCLATURE

a_m	Catalyst's surface-volume relation, $m^2\ m^{-3}$
C_A	A compound's concentration in stream, mol m^{-3} o ppm
C_{A0}	A compound's concentration in feed stream, mol m^{-3} o ppm
C_{AS}	A compound's concentration in catalyst's surface, mol m^{-3} or ppm
C_p	Heat capacity, J kg^{-1} $^oC^{-1}$
D_{AB}	Diffusion coefficient of gas A in gas B, $cm^2\ s^{-1}$
D_E	Effective diffusion coefficient, $m^2\ s^{-1}$
d_P	Catalyst particle's diameter, mm
d_{pore}	Average size of catalyst's pores, m
F_{A0}	Inlet molar flow of A compound, mol h^{-1}
h_C	Convective heat transmission coefficient, J s^{-1} m^{-2} $^oC^{-1}$
k'	Potential kinetics reaction constant, (depends on equation) 1^{st} order: $m^3\ g^{-1}\ h^{-1}$
k	Conductive heat transmission coefficient, J s^{-1} m^{-1} $^oC^{-1}$
k_C	Mass transfer coefficient, m s^{-1}
k^M	Mechanistic kinetic reaction constant, (depends on equation)
K	Adsorption constant, (depends on equation)
L	Total length of catalyst's pore, m
M_A, M_B	Molar weight of A or B, g mol^{-1}
n	Order of chemical reaction
Nu	Nusselt's dimensionless number
P	Pressure, bar
P_0	Vapour pressure, bar
Pr	Prandtl's dimensionless number
Q	Volumetric flow rate, l_S min^{-1}
Q_C	Convective heat flow, J s^{-1}
$-r_A$	Reaction rate, mol h^{-1} g^{-1}
$(-r_A)_{obs}$	Observed reaction rate, mol h^{-1} g^{-1}
Re	Reynolds' dimensionless number
R_{Pore}	Catalyst's pore's radius, m
r_P	Catalyst particle's radius, m
Sc	Schmit's dimensionless number
Sh	Sherwood's dimensionless number
T	Temperature, ^oC or K
T_{bed}	Temperature in the catalyst fixed bed, ^oC
T_{flow}	Temperature in the outlet of the fixed bed, ^oC
u	Linear velocity, m s^{-1}
V_m	Molecular volume, $cm^3\ mol^{-1}$
V_P	Catalyst's pores volume, $m^3\ kg^{-1}$
W	Catalysts mass, g
w_P	Weight of catalyst particle, g $part.^{-1}$
W/F_{A0}	Space or residence time, g h mol^{-1}
x	Position in the catalyst's pore
x_A	Conversion of reagent A

6.1 GREEK LETTERS AND SYMBOLS

$\alpha, \beta, \gamma, \delta, \zeta, \kappa$	Reaction order in mechanistic kinetics
ΔD	Incremental of pore diameter, Å
ΔT	Temperature difference between the catalytic bed and reactor's outlet, ºC
ΔV	Increment of pore volume, $cm^3\ g^{-1}$
Δx	Incremental of position in the catalyst's pore, m
ε_C	Catalyst's porosity
η	Efficiency factor
μ_A	viscosity of A, P
μ_∞	viscosity in stream, P
μ_S	viscosity at catalyst's surface, P
ρ_A	Density of A gas, $kg\ m^{-3}$
ρ_c	Catalyst's density, $kg\ m^{-3}$
ρ_L	Fixed bed's apparent density, $kg\ m^{-3}$
ρ_S	Support's density, $kg\ m^{-3}$
τ_C	Catalyst's tortuosity
ϕ	Thiele's modulus

6.2 ACHRONYMS AND ABBREVIATIONS

2,3,7,8-TCDB	2,3,7,8-Tetrachlorodibenzodioxin
APCD	Air Pollution Control Devices
BET	Brunauer Emmet Teller
BJH	Barrett Joyner Halenda
CTO	Catalytic Total Oxidation
deDin	Technology for elimination of PCDD/PCDFs
deDiNox	Technology for simultaneous elimination of PCDD/PCDFs and NO_X
deNO_X	Techonolgy for elimination of NO_X
ER	Eley Rideal
IUPAC	International Union of Pure and Applied Chemistry
LH	Langmuir Hinshelwood
MSW	Municipal Solid Waste
MVK	Mars Van Krevelen
MWI	Municipal Waste Incinerator
NO_x	Nitrogen's oxides
o-DCB	1,2-dichlorobenzene
PAH	Polycyclic Aromatic Hydrocarbon
PCDD	Polichlorinated dibenzodioxins
PCDF	Polichlorinated dibenzofurans
RSD	Relative Standard Deviation
STP	Standard Temperature and Pressure (0 ºC, 1 bar). Used as a subscript: "S"
SCR	Selective Catalytic Reduction
VO_X/TiO_2	Vanadia based catalyst supported on titania
WTE	Waste to Energy

7 REFERENCES

Albonetti, S., Blasioli, S., Bonelli, R., Epoupa Mengou, J., Scirè, S., Trifirò, F, 2008. The role of acidity in the decomposition of 1,2-dichlorobenzene over TiO_2-based V_2O_5/WO_3 catalysts. Applied Catalysis A: General 341: 18-25.

Bertinchamps, F., Treinen, M., Blangenois, N., Mariage, E., Gaigneaux, E.M., 2005. Possitive effect of NO_X on the performances of VO_X/TiO_2-based catalysts in the total oxidation abatement of chlorobenzene. Journal of Catalysis 230: 493-498.

Brunner, C.R., 1994. Hazardous Waste Incineration. 2nd edition. New York: McGraw-Hill.

Busca, G., Lietti, L., Ramis, G., Berti, F., 1998. Chemical and mechanistic aspects of the selective catalytic reduction of NO_X by ammonia over oxide catalysts: A review. Applied Catalysis B: Environmental 18: 1-36.

Davis, M.E., Davis, R.J., 2003. Chapter 6 - Effects of Transport Limitations on Rates of Solid-Catalyzed Reactions. In Fundamentals of chemical reaction engineering, by M.E., Davis, R.J. Davis, 184-239. New York: McGraw-Hill.

Debecker, D.P., Bertinchamps, F., Blangenois, N., Eloy, P., Gaigneaux, E.M., 2007. On the impact of the choice of model VOC in the evaluation of V-based catalysts for the total oxidation of dioxins: Furan vs. chlorobenzene. Applied Catalysis B: Environmental 74: 223-232.

Directive 2000/76/EC of the European Parliament and of the Council of 4th December 2000 on the incineration of waste, 2000.

Dvorák, R., Chlápek, P., Jecha, D., Puchýr, R., Stehlík, P., 2010. New approach to common removal of dioxins and NO_X as a contribution to environmental protection. Journal of a Cleaner Production 18: 881-888.

Economidis, N.V., Peña, D.A., Smirniotis, P.G., 1999. Comparison of TiO_2-based oxide catalysts for the selective catalytic reduction of NO: effect of aging the vanadium precursor solution. Applied Catalysis B: Environmental 23: 123-134.

Finocchio, E., Busca, G., Notaro, M., 2006. A review of catalytic processes for the desctruction of PCDD and PCDF from waste gases. Applied Cartalysis B: Environmental 62: 12-20.

Fogler, H.S., 2005. Elements of Chemical Reaction Engineering (4th edition). Prentice Hall.

Forzatti, P., Nova, I., Tronconi, E., Kustov, A., Reimer Thogersen, J., 2012. Effect of operating variables on the enhanced SCR reaction over a commercial V_2O_5-WO_3/TiO_2 catalyst for stationary applications. Catalysis today 184: 153-159.

Gallastegi-Villa, M., Aranzabal, A., Boukha, Z., González-Marcos, J.A., González-Velasco, J.R., Martínez-Huerta, M.V., Bañares, M.A., 2015. Role of surface vanadium oxide coverage support on titania for the simultaneous removal of o-dichlorobenzene and NO_X from waste incinerator flue gas. Catalysis Today.

Gannoun, C., Delaigle, R., Debecker, D.P., Eloy, P., Ghorbel, A., Gaigneaux, E.M., 2012. Effect of support on V_2O_5 catalytic activity in Chlorobenzene oxidation. Applied Catalysis A: General.

Goemans, M., Clarysse, P., Joannès, J., De Clerq, P., Lenaerts, S., Matthys, K., Boels, K., 2003. Catalytic NO_X reduction with simultaneous dioxin and furan oxidation." Chemosphere 50: 489-497.

González-Velasco, J.R., González-Marcos, J.A., González-Marcos, M.P., Gutiérrez-Ortiz, J.I., Gutiérrez-Ortiz, M.A., 1999. Cinética Química aplicada. Madrid: Síntesis.

Green, D.W., Perry, R.H., 2008. Heat and Mass Transfer. In Perry's Engineer's Handbook, by D.W. Green and Perry, R.H. McGraw-Hill.

Hou, Y., Cai, G., Huang, Z., Han, X., Guo, S., 2014. Effect of HCl on V_2O_5/AC catalyst for NO reduction by NH_3 at low temperatures. Chemical Engineering Journal 247: 59-65.

Jones, J., Ross, J.R.H., 1997. The development of supported vanadia catalysts for the combined catalytic removal of the oxides of nitrogen and of chlorinated hydrocarbons from flue gases. Catalysis Today 35: 97-105.

Krishnamoorthy, S., Baker, J.P., Amiridis, M.D., 1998. Catalytic oxidation of 1,2-dichlorobenzene over V_2O_5/TiO_2 catalysts. Catalysis Today 40: 39-46.

McKay, G., 2002. Dioxin characterisation, formation and minimisation during municipal solid waste (MSW) incineration: review. Chemical Engineering Journal 86: 343-368.

Mears, D.E., 1971. Tests for Transport Limitations in Experimental Catalytic Reactors. Industrial & Engineering Chemistry Process Design and Development 10: 541-547.

Nakajima, F., Hamada, I., 1996. The-state-of-the-art technology of NO_X control. Catalysis today 29: 109-115.

Schimmoeller, B., Delaigle, R., Debecker, D.P., Gaigneaux, E.M., 2010. Flame-made vs. wet-impregnated vanadia/titania in the total oxidation of chlorobenzene: Possible role of VO_X species. Catalysis today 157: 198-203.

Stoll, M., Furrer, J., Seifert, H., Schaub, G., Unruh, D., 2001. Effects of flue gas composition on the catalytic destruction of chlorinated aromatic compounds with a V-oxide catalyst. Waste Management 21: 457-463.

Su, G., Huang, L., Liu, S., Lu, H, Yang, F., Zheng, M., 2015. The combined disposal of 1,2,4-trichlorobenzene and nitrogen oxides using synthesized $Ce_{0.2}TiAl_{\alpha}O_X$ micro/nanomaterial. Catalysis science & technology 5: 1041.

Vielstich, W., Gasteiger, H.A., Yokokawa, H., Lamm, A., 2003. Handbook of fuel cells: fundamentals, technology and applications. Chichester, England: Wiley.

Wang, J., Wang, X., Liu, X., Zeng, J., Guo, Y., Zhu, T., 2015. Kinetics and mechanism study on catalytic oxidation of chlorobenzene over V_2O_5/TiO_2 catalysts." Journal of Molecular Catalysis A: Chemical 402: 1-9.

Wielgosinski, G., Grochowalski, A., Machej, T., Pajak, T., Cwiakalski, W., 2007. Catalytic destruction of 1,2-dichlorobenzene on V_2O_5-WO_3/Al_2O_3-TiO_2 catalyst. Chemosphere 67: 150-154.

Wu, M., Chol Ung, K., Dai, Q., Wang, X., 2012. Catalytic combustion of chlorinated VOCs over VO_X/TiO_2 catalysts. Catalysis Communications 18: 72-75.

Xu, Z., Deng, S., Yang, Y., Zhang, T., Cao, Q., Huang, J., Yu, G., 2012. Catalytic destruction of pentachlorobenzene in simulated flue gas by a V_2O_5-WO_3/TiO_2 catalyst. Chemosphere 87: 1032-1038.

Xue, W., Jian, W., Tingyu, Z., 2013. Coupled Control of Chlorobenzene and NO over V_2O_5/TiO_2 Catalyst in NH_3-SCR Reaction. Advanced Materials Research 811: 83-86.